THE PENNSYLVANIA
STATE UNIVERSITY

A MOVABLE MASS CONTROL SYSTEM TO DETUMBLE A DISABLED SPACE VEHICLE

BY
TERRY L. EDWARDS

ASTRONAUTICS RESEARCH REPORT
NO. 73-5

DEPARTMENT OF AEROSPACE ENGINEERING
UNIVERSITY PARK, PENNSYLVANIA

RESEARCH SUPPORTED BY NASA GRANT NGR 39-009-210

ACKNOWLEDGEMENTS

The author wishes to express his gratitude to Dr. Marshall H. Kaplan, Associate Professor of Aerospace Engineering, for his invaluable suggestions and guidance of this work.

The work reported in this thesis was sponsored by the National Aeronautics and Space Administration, through grant number NGR 39-009-210.

TABLE OF CONTENTS

LIST OF TABLES

LIST OF FIGURES

LIST OF FIGURES (Continued)

NOMENCLATURE

a,b	Mass track offset distances
$\vec{a}$	Inertial acceleration of reference point
A_n,B_n	Fourier series coefficients (n = 1, 2, ...)
c_1,c_2	Control law parameters
$\vec{f}$	Force applied to the control mass and reacted to by the vehicle
$\vec{F}$	External force applied to system
F	Forcing function of mass equation of motion
$\vec{H}$	Total angular momentum of system relative to main body center of mass
$\vec{H}_b$	Angular momentum of main body relative to its own center of mass
$\vec{H}_c$	Total angular momentum of system relative to composite center of mass
$\vec{H}_m$	Angular momentum of control mass relative to the main body center of mass treated as point mass
I_1,I_2,I_3	Principal moments of inertia of main vehicle
k	Modulus of Jacobian elliptic functions
m	Mass of control mass
M	Mass of main vehicle
$\vec{M}$	External moment acting on system
p	Precessional frequency
$\vec{r}$	Position vector of control mass relative to main vehicle center of mass
$\vec{S}$	First moment of mass of the system
T	Total kinetic energy of the system
T_{rot}	Rotational kinetic energy of the system

NOMENCLATURE (Continued)

$\dot{T}_{sec}$	Secular part of the rate of change of rotational kinetic energy
x,y,z	Components of $\vec{r}$ in body-fixed reference frame
z_{max}	Maximum amplitude of control mass oscillation
α,β,γ	Amplitudes of angular rotation rates
θ	Wobble angle
μ	Reduced mass = $\frac{mM}{m+M}$
τ	Period of forcing function of equation of mass motion
τ_c	Time constant associated with stabilizing performance of the control system
$\vec{\omega}$	Angular velocity vector of main body with components ω_1, ω_2, ω_3

CHAPTER I.

INTRODUCTION

In the operation of future manned space vehicles there is always a finite probability that an accident will occur which results in uncontrolled tumbling of a spacecraft. This uncontrolled motion creates a hazardous environment to the crew, which would experience oscillating accelerations. The structural integrity of the disabled vehicle may be jeopardized by prolonged tumbling presenting additional danger. An earth-launched rescue vehicle may not arrive for approximately twenty-four hours due to fueling, launching, and rendezvous operations. Hard docking by a manned rescue craft with the disabled vehicle is not possible because of the hazardous environment to which the rescue crew would be exposed and the excessive accelerations and fuel usage required of the rescue vehicle. Detumbling would then have to be accomplished by an external means using a remotely controlled tele-operator or by impinging fluid jets on the disabled craft. Therefore, it is desirable to develop an internal autonomous control system to either completely detumble the vehicle or lessen the tumbling motions until the rescue craft arrives. Such a device would become active upon loss of control.

Mass expulsion devices require onboard storage of propellant and, hence, may not be reliable for this application on a long term basis. Momentum exchange devices, such as control moment gyros, may require continuous operation since startup of the gyros would be difficult once a tumbling situation has occurred. Power requirements for continuous operation of this safety device may be prohibitive. Control moment gyros experience a marked increase in gimbal loading in a tumbling vehicle and would be subject to gimbal failures. These devices also have a tendency for saturation in large corrective maneuvers. Passive energy dissipation devices such as viscous ring and pendulum dampers are reliable and simple but have relatively low energy dissipation rates, and therefore, require a long time for stabilization. These devices seem most appropriate for vehicles which have a high nominal spin rate about one axis. For this application passive devices can effectively damp out relatively small transverse rates. However, an emergency detumbling system should be capable of stabilizing a disabled vehicle with arbitrary tumbling motions where all angular velocities may be of the same order of magnitude.

The development of a movable mass control system to convert the tumbling motions of a disabled vehicle into simple spin is presented here. A simple spin state would

greatly facilitate crew evacuation and final despinning by an external means. The system moves a control mass, according to a selected control law, in the acceleration environment created by the tumbling motion. By moving the mass properly, the rotational kinetic energy of the system may be increased or decreased creating simple spin states about the minimum or maximum moment of inertia axis, respectively. The control system is designed for the latter case due to its associated stability in the presence of perturbing forces.

The complete equations of motion of a rigid spacecraft with attached control mass are formulated making no assumptions concerning vehicle symmetry or magnitude of the transverse angular rates. A control law relating control mass motions to vehicle motions is selected based on Liapunov stability theory. A method of determining control system parameter values, based on an estimate of the worst case tumble state, is also presented. For a large space station and realistic initial conditions, it is shown that the movable mass control system is capable of decreasing the kinetic energy of the system to its minimum state, establishing a simple spin about the maximum moment of inertia axis, in several hours. An additional application of a movable mass control system as a wobble damper for an artificial-g mode space station is also presented. Finally, comparisons with competitive passive devices for this application are made.

CHAPTER II

PREVIOUS INVESTIGATIONS

The effect of internal moving parts on the attitude motions of a space vehicle has been investigated by Roberson (1) and Grubin (2). Both of these authors have developed the equations of motion of a rigid main body carrying an arbitrary number of moving rigid bodies. These studies are primarily concerned with analytically describing the result of internal mass motion so that possible destabilizing effects may be determined. Roberson chose the composite center of mass of the system as the reference point for the equations of motion. For this choice of reference point, the formulation leads to time varying moments of inertia of the main vehicle since the reference point is moving relative to the vehicle due to mass motion. Grubin circumvented this problem by choosing the center of mass of the vehicle as the reference point for the equations of motion. For this choice, the moments of inertia of the vehicle are constant relative to a body fixed coordinate system. As noted by Grubin, the formulation may produce equations of motion which are no simpler than those produced by Roberson's method. However, the selection of the vehicle center of mass as the reference point seems more natural since the rotational motions of the spacecraft may be referred directly to the vehicle center of mass rather

than the moving composite center of mass of the system. In addition, the motion of the moving mass may be expressed relative to the vehicle axes which is of some practical advantage.

Kane and Sobala (3) investigated the possibility of using the effect of internal mass motion to provide attitude stabilization. The system considered was a symmetric satellite and two particles performing prescribed oscillations. The particles were constrained to move along the axis of symmetry. In a later paper Kane and Scher (4) discussed the possibility of moving the parts of a connected system relative to each other to convert undesirable tumbling or nutation into simple spin. The proposed concept exploits the following facts. When the system is constrained to move as a single rigid body, the rotational kinetic energy is constant and bounded between two limits. These limits are determined by the angular momentum and the maximum and minimum moments of inertia of the system. If the parts of the system are moved relative to each other and again constrained to form a rigid body, the rotational kinetic energy of the new configuration will, in general, be different from the initial value. Therefore, the control scheme presented by Kane and Scher is to move the parts relative to each other in such a way that the rotational kinetic energy changes to its maximum or minimum value. The system

would then be in a simple spin state about either the minimum or maximum moment of inertia axis. However, Kane and Scher do not present a general control law to accomplish this stabilization technique. It is suggested that a catalog of control laws be compiled for use with various tumble states. Then, once a tumble state has been identified, the proper control law may be selected for this case.

Childs (5) developed a movable mass control system for an artificial-g space station. The analysis is not dependent on vehicle symmetry but the assumptions of a high nominal spin rate about one axis and small transverse rates are made. This allows Childs to linearize the equations of motion and formulate a relatively simple control law. However, the control system does not damp the transverse rates to zero but only to a constant value. This does not completely detumble the vehicle but does reduce the disturbance that crew members would experience.

Beachley (6) suggested another application for movable masses. He has shown that the inversion of a spin-stabilized spacecraft may be accomplished using movable masses. The concept involves moving the masses to make the spin axis unstable by changing the moments of inertia of the system. This will cause the cone angle between the angular momentum vector and the line of

symmetry to increase. As the spacecraft completes the inversion phase the control masses are returned to their original position. The inverted spacecraft will again be spinning in a stable manner.

Lorell and Lange (7) have proposed using two pairs of movable masses to provide an automatic mass trim system for a spinning spacecraft. For an active control system, the accuracy of the pointing control depends on knowledge of the relative location of the spin axis and the sensor axis. If the spin axis shifts and the spin and sensor axes are not correctly aligned, a pointing error arises which is difficult to eliminate. Therefore, Lorell and Lange propose a movable mass system to trim the location of the spin axis to align the sensor and spin axes. The analyses presented is limited to the assumption of a symmetric vehicle and small transverse rates.

These previous investigations have used movable masses for a variety of applications. However, most of these applications have been developed for vehicles which are symmetric or experience only small transverse rotation rates which permits some degree of linearization. Available literature indicates that a movable mass control system has not been developed for the general case of an asymmetric vehicle with arbitrarily large rotation rates about each axis.

CHAPTER III

ANALYTICAL INVESTIGATIONS

Development of Equations of Motion

The complete equations of motion of a rigid spacecraft with an attached mass are developed in this section. In the following analyses $\dot{\vec{v}}$ implies differentiation with respect to an inertial reference frame and $[\dot{\vec{v}}]$ implies differentiation relative to a body fixed reference frame.

The generalized equation of motion for a system of connected rigid bodies is given by Grubin (2) as

$$\vec{M} = \dot{\vec{H}} + \vec{S} \times \vec{a} \tag{1}$$

where $\vec{M}$, $\vec{H}$, and $\vec{S}$ denote the external moment, angular momentum, and first moment of mass of the system, respectively. The quantities are specified with respect to an arbitrary reference point moving in an arbitrary manner. The inertial acceleration of the reference point is $\vec{a}$. This equation reduces to the standard form, $\vec{M} = \dot{\vec{H}}$, when the reference point is fixed ($\vec{a} = 0$) or is the center of mass of the system ($\vec{S} = 0$).

The system under consideration consists of a rigid main body and attached control mass shown in Figure 1. The reference point for the equation of motion is selected as the center of mass of the main body. The body fixed coordinate system is aligned with the principal axes of

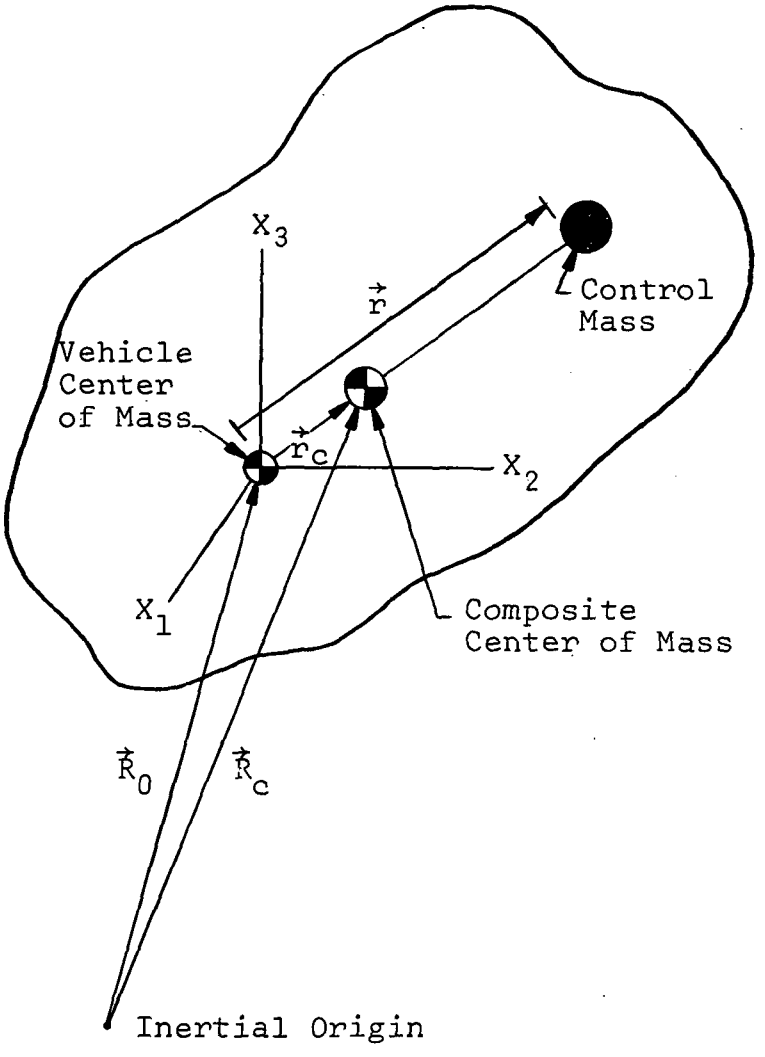

Figure 1. Main Body and Attached Mass System Geometry

the vehicle, X_1, X_2, and X_3, and have associated unit vectors $\hat{i}$, $\hat{j}$, and $\hat{k}$, respectively.

With the assumption of no applied external torques, Equation 1 becomes

$$\dot{\vec{H}} + \vec{S} \times \vec{a} = 0 \tag{2}$$

where $\vec{H}$ is the total angular momentum of the system.

$$\vec{H} = \vec{H}_b + \vec{H}_m \tag{3}$$

The angular momentum of the main body, $\vec{H}_b$, is

$$\vec{H}_b = I_1\omega_1\hat{i} + I_2\omega_2\hat{j} + I_3\omega_3\hat{k} \tag{4}$$

where I_1, I_2, and I_3 are the principal moments of inertia of the vehicle without the control mass and ω_1, ω_2, and ω_3 are the rotation rates about the X_1, X_2, and X_3 axes, respectively. Differentiating this equation yields

$$\begin{aligned}\dot{\vec{H}}_b &= [\dot{\vec{H}}_b] + \vec{\omega} \times \vec{H} \\ &= [I_1\dot{\omega}_1 + \omega_2\omega_3(I_3 - I_2)]\hat{i} \\ &+ [I_2\dot{\omega}_2 + \omega_1\omega_3(I_1 - I_3)]\hat{j} \\ &+ [I_3\dot{\omega}_3 + \omega_1\omega_2(I_2 - I_1)]\hat{k}\end{aligned} \tag{5}$$

The angular momentum of the control mass relative to the vehicle center of mass, $\vec{H}_m$, is

$$\vec{H}_m = m\vec{r} \times \dot{\vec{r}} \tag{6}$$

It has been assumed that the control mass is essentially a point mass so that the angular momentum of the mass about its own axes may be neglected. The rate of change of angular momentum of the mass is then

$$\dot{\vec{H}}_m = m\vec{r} \times \ddot{\vec{r}}. \tag{7}$$

The term $\ddot{\vec{r}}$ is the acceleration of the control mass relative to the main body center of mass. From Thomson (8), this acceleration may be written as

$$\ddot{\vec{r}} = \vec{\omega} \times (\vec{\omega} \times \vec{r}) + \dot{\vec{\omega}} \times \vec{r} + 2\vec{\omega} \times [\dot{\vec{r}}] + [\ddot{\vec{r}}]. \tag{8}$$

The first term is the centripetal acceleration, the second is the tangential acceleration, the third is the Coriolis acceleration, and the last term is the acceleration relative to the body fixed reference frame.

The first moment of mass of the system is given by

$$\vec{S} = m\vec{r} = m(x\hat{i} + y\hat{j} + z\hat{k}). \tag{9}$$

Note that the main body does not contribute to this term since the reference point is the center of mass of the vehicle.

The inertial acceleration of the reference point is

$$\vec{a} \triangleq \ddot{\vec{R}}_0$$

and, from Figure 1, may be written as

$$\vec{a} = \ddot{\vec{R}}_c - \ddot{\vec{r}}_c.$$

The term $\ddot{\vec{R}}_c$ is the inertial acceleration of the composite center of mass of the system and is given as

$$\ddot{\vec{R}}_c \triangleq \frac{\vec{F}}{M + m}.$$

Here $\vec{F}$ is the resultant of the external forces acting on the system, M is the mass of the main body, and m is mass of the control mass. With the assumption of no external forces acting on the system, $\ddot{\vec{R}}_c = 0$. Also, from the definition of center of mass of the system

$$\vec{r}_c = \frac{m}{m + M} \vec{r} \tag{10}$$

so that the acceleration of the reference point becomes

$$\vec{a} = -\frac{m}{m + M} \ddot{\vec{r}}.$$

Inserting these relations into Equation 2 yields

$$\dot{\vec{H}}_b + \frac{mM}{m + M} \vec{r} \times \ddot{\vec{r}} = 0. \tag{11}$$

Defining the reduced mass of the system as

$$\mu \triangleq \frac{mM}{m + M}$$

and identifying

$$\vec{f} = \mu \ddot{\vec{r}} \tag{12}$$

as the force applied to the control mass and reacted to by the vehicle, Equation 11 becomes

$$\dot{\vec{H}}_b = -\vec{r} \times \vec{f}. \tag{13}$$

For prescribed motions of the control mass, this relation gives, in vector form, the equation of motion of the vehicle. It is evident that the dynamics may be considered to be those of a rigid body being acted on by a reaction moment of $-\vec{r} \times \vec{f}$ which is a result of mass motion.

Expanding Equation 13 yields a set of three coupled, non-linear differential equations for the vehicle dynamics in terms of the vehicle angular rates (ω_1, ω_2, ω_3), and the movable mass position (x, y, z), velocity ($\dot{x}$, $\dot{y}$, $\dot{z}$), and acceleration ($\ddot{x}$, $\ddot{y}$, $\ddot{z}$). All of these quantities are with respect to the body fixed principal axes (X_1, X_2, X_3, respectively). The equations are:

$$[I_1 + \mu(y^2 + z^2)]\dot{\omega}_1 + [I_3 - I_2 + \mu(y^2 - z^2)]\omega_2\omega_3 + \mu[-xy\dot{\omega}_2 - xz\dot{\omega}_3 + (2y\dot{y} + 2z\dot{z})\omega_1 + yz(\omega_3^2 - \omega_2^2) - 2\dot{x}y\omega_2 - 2\dot{x}z\omega_3 - xz\omega_1\omega_2 + xy\omega_1\omega_3 + y\ddot{z} - z\ddot{y}] = 0 \quad (14)$$

$$[I_2 + \mu(z^2 + x^2)\dot{\omega}_2 + [I_1 - I_3 + \mu(z^2 - x^2)]\omega_3\omega_1 + \mu[-yz\dot{\omega}_3 - yx\dot{\omega}_1 + (2z\dot{z} + 2x\dot{x})\omega_2 + zx(\omega_1^2 - \omega_3^2) - 2\dot{y}z\omega_3 - 2\dot{y}x\omega_1 - yx\omega_2\omega_3 + yz\omega_2\omega_1 + z\ddot{x} - x\ddot{z}] = 0 \quad (15)$$

$$[I_3 + \mu(x^2 + y^2)\dot{\omega}_3 + [I_2 - I_1 + \mu(x^2 - y^2)]\omega_1\omega_2$$

$$+ \mu[-zx\dot{\omega}_1 - zy\dot{\omega}_2 + (2x\dot{x} + 2y\dot{y})\omega_3 + xy(\omega_2^2 - \omega_1^2)$$

$$- 2\dot{z}x\omega_1 - 2\dot{z}y\omega_2 - zy\omega_3\omega_1 + zx\omega_3\omega_2 + x\ddot{y} - y\ddot{x}]$$

$$= 0 \tag{16}$$

These equations are valid irrespective of the physical mechanism whereby the control mass executes its motions.

Similarly, the force, $\vec{f}$, applied to the control mass and reacted to by the vehicle, given by Equation 12, may be expanded in component form. The result is

$$f_1 = \mu[\ddot{x} - 2\dot{y}\omega_3 + 2\dot{z}\omega_2 - y\dot{\omega}_3 + z\dot{\omega}_2 + y\omega_1\omega_2$$

$$+ z\omega_1\omega_3 - x(\omega_2^2 + \omega_3^2)] \tag{17}$$

$$f_2 = \mu[\ddot{y} - 2\dot{z}\omega_1 + 2\dot{x}\omega_3 - z\dot{\omega}_1 + x\dot{\omega}_3 + z\omega_2\omega_3$$

$$+ x\omega_2\omega_1 - y(\omega_3^2 + \omega_1^2)] \tag{18}$$

$$f_3 = \mu[\ddot{z} - 2\dot{x}\omega_2 + 2\dot{y}\omega_1 - x\dot{\omega}_2 + y\dot{\omega}_1 + x\omega_3\omega_1$$

$$+ y\omega_3\omega_2 - z(\omega_1^2 + \omega_2^2)]. \tag{19}$$

The kinetic energy of the system is

$$T = \frac{1}{2}\int^M \dot{\vec{\xi}} \cdot \dot{\vec{\xi}}\, dm + \frac{1}{2}m\dot{\vec{R}}_m \cdot \dot{\vec{R}}_m. \tag{20}$$

From Figure 2 the following relations are evident.

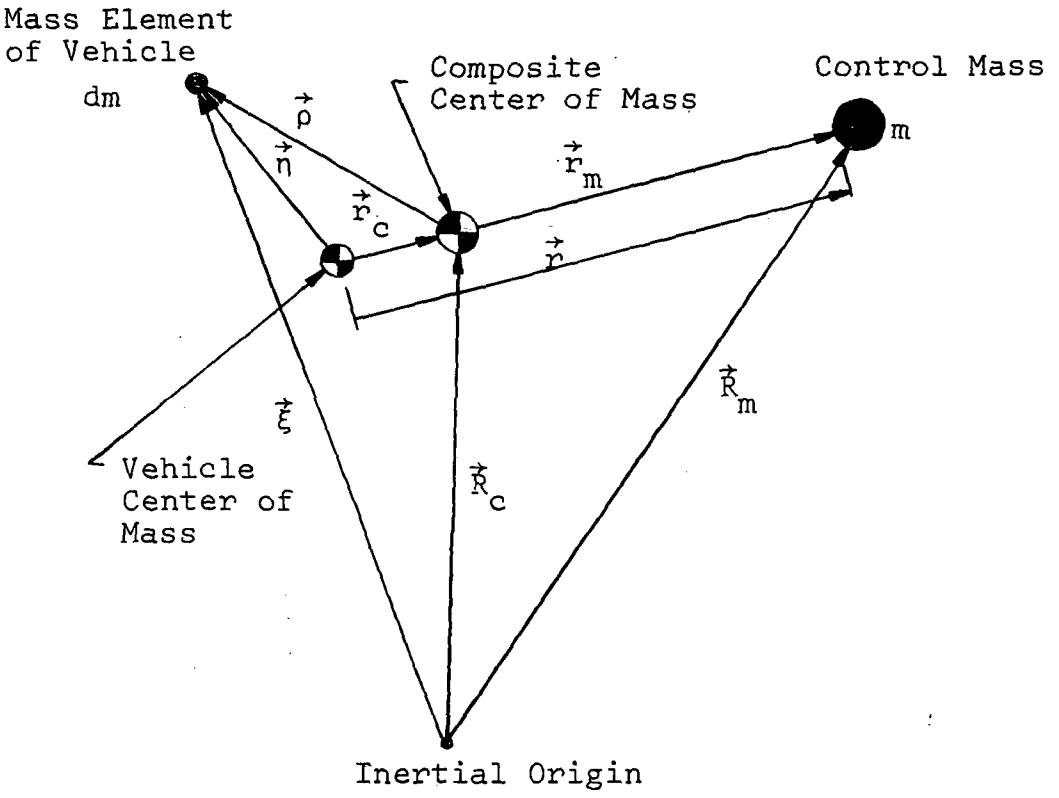

Figure 2. System Geometry for Determination of System Kinetic Energy

$$\vec{\xi} = \vec{R}_c + \vec{\rho}$$

$$\vec{R}_m = \vec{R}_c + \vec{r}_m$$

Inserting these relations into Equation 20 yields

$$T = \frac{1}{2}(m + M)\dot{\vec{R}}_c \cdot \dot{\vec{R}}_c + (\frac{1}{2}\int^M \dot{\vec{\rho}} \cdot \dot{\vec{\rho}}\, dm + \frac{1}{2}m\dot{\vec{r}}_m \cdot \dot{\vec{r}}_m) + \dot{\vec{R}}_c \cdot (\int^M \dot{\vec{\rho}}\, dm + m\dot{\vec{r}}_m).$$

The first term may be identified as the kinetic energy associated with the motion of the composite center of mass of the system. The second grouping of terms is the rotational kinetic energy about the composite center of mass. The final terms are zero from the definition of center of mass of the system. Since only attitude motions of the system are of interest, only the rotational kinetic energy will be considered further.

$$T_{rot} = \frac{1}{2}\int^M \dot{\vec{\rho}} \cdot \dot{\vec{\rho}}\, dm + \frac{1}{2}m\dot{\vec{r}}_m \cdot \dot{\vec{r}}_m \qquad (21)$$

Again from Figure 2

$$\vec{r}_m = \vec{r} - \vec{r}_c$$

and

$$\vec{\rho} = \vec{\eta} - \vec{r}_c.$$

Using these relations and Equation 10, the rotational kinetic energy of the system becomes

$$T_{rot} = \frac{1}{2}\int^M \dot{\vec{\eta}} \cdot \dot{\vec{\eta}}\, dm + \frac{1}{2}\frac{mM}{m + M}\dot{\vec{r}} \cdot \dot{\vec{r}}. \qquad (22)$$

The first term of this equation is the rotational kinetic energy of the rigid body about its own center of mass. The second term is the kinetic energy of the reduced mass about the vehicle center of mass. Therefore, the rotational kinetic energy of the system about the composite center of mass may be written as

$$T_{rot} = \frac{1}{2}\vec{\omega} \cdot \overline{\overline{I}} \cdot \vec{\omega} + \frac{1}{2}\mu\dot{\vec{r}} \cdot \dot{\vec{r}} \tag{23}$$

where $\overline{\overline{I}}$ is the inertia dyadic of the rigid body. It is interesting to note that the rotational kinetic energy of the system given by Equation 23 is valid irrespective of the choice of a body fixed principal axis coordinate system.

The expression for the angular momentum of the system with respect to the composite center of mass may be developed similarly. The result is, from Roberson (1),

$$\vec{H}_c = \overline{\overline{I}} \cdot \vec{\omega} + \mu\vec{r} \times \dot{\vec{r}}. \tag{24}$$

It should be remembered that $\vec{H}$ in Equation 3 is the angular momentum with respect to the vehicle center of mass, whereas $\vec{H}_c$ in Equation 24 is the angular momentum with respect to the composite center of mass of the system. The equation of motion would be

$$\dot{\vec{H}}_c = 0 \tag{25}$$

if the composite center of mass were selected as the reference point for Equation 1. Since Equation 25 indicates that H_c is constant, the accuracy of a numerical solution of the equations of motion may be determined using Equation 24.

Since the movable mass control system is to decrease the rotational kinetic energy of the system, the rate of change of this energy will be developed. Differentiating Equation 23 yields

$$\dot{T}_{rot} = \vec{\omega} \cdot \bar{\bar{I}} \cdot \dot{\vec{\omega}} + \dot{\vec{r}} \cdot \vec{f}. \tag{26}$$

Partially expanding Equation 13 gives

$$\bar{\bar{I}} \cdot \dot{\vec{\omega}} + \vec{\omega} \times \bar{\bar{I}} \cdot \vec{\omega} = -\vec{r} \times \vec{f}$$

so that

$$\vec{\omega} \cdot \bar{\bar{I}} \cdot \dot{\vec{\omega}} = -\vec{\omega} \cdot \vec{\omega} \times \bar{\bar{I}} \cdot \vec{\omega} - \vec{\omega} \cdot \vec{r} \times \vec{f}.$$

It may be noted that the first term on the right hand side of this equation is zero. Using this relation, Equation 26 becomes

$$\dot{T}_{rot} = -\vec{\omega} \cdot \vec{r} \times \vec{f} + \dot{\vec{r}} \cdot \vec{f}.$$

Noting that

$$\dot{\vec{r}} = [\dot{\vec{r}}] + \vec{\omega} \times \vec{r}$$

this equation simplifies to the result

$$\dot{T}_{rot} = [\dot{\vec{r}}] \cdot \vec{f}. \tag{27}$$

Thus, the rate of change of rotational kinetic energy of the system is found to be independent of the vehicle inertia properties and dependent only on the relative velocity of the control mass and the force applied to the mass. It may be noted that this result is valid irrespective of the assumption of a principal axis coordinate system since Equations 13 and 23 are general.

The equations of motion of a rigid spacecraft with attached control mass have been formulated in this section. The result is a set of three coupled, non-linear differential equations for the rotation rates of the vehicle in terms of the control mass position, velocity, and acceleration. The motion of the control mass will be specified by the control law which is selected. The expression for the angular momentum of the system about the composite center of mass has been presented to determine the accuracy of a numerical solution of the equations of motion. Since the movable mass control system is to provide energy dissipation, the expressions for the rotational kinetic energy of the system and the rate of change of this quantity have been developed. The derived relation for the rate of change of rotational kinetic energy will be used to develop a control law in the next section.

Selection of Control Law

Equations 14-16 determine the attitude motions of the spacecraft for specified motions of the control mass. It is the function of the control law to relate the motions of the control mass to measurable vehicle parameters so that the control mass may respond to vehicle motions in an appropriate manner to lessen tumbling. A satisfactory control law should not be unnecessarily complicated and should not have excessive power or sensor requirements. It should, however, require determination of only measurable vehicle parameters, produce stable responses, and result in a final state of a simple spin about either the maximum or minimum moment of inertia axis. In the following analysis, the vehicle is assumed to have three distinct moments of inertia, I_1, I_2, and I_3, and the relationship $I_3 > I_2 > I_1$ is assigned to these quantities.

By inspection of Equations 14-16, the equations of motion for an asymmetric vehicle with attached movable mass are extremely complicated due to their highly coupled and non-linear nature. Since the initial tumble rates may be large about all three axes, the equations of motion cannot be simplified by linearization. However, several simple cases were identified and will be discussed before considering the general case.

The first special case requires that the motion of the mass be along a line parallel to and offset a distance b from the X_3 axis and passing through the X_2 axis. For this case, Equation 14 becomes

$$[I_1 + \mu(b^2 + z^2)]\dot{\omega}_1 + [I_3 - I_2 + \mu(b^2 - z^2)]\omega_2\omega_3 + 2\mu z\dot{z}\omega_1 + \mu bz(\omega_3^2 - \omega_2^2) + \mu b\ddot{z} = 0. \quad (28)$$

Suppose the control law is chosen such that

$$z = c\omega_1. \quad (29)$$

With the assumption, $I_1 >> 3\mu c^2\omega_1^2$, Equation 28 becomes

$$\ddot{\omega}_1 + \frac{[I_1 + \mu b^2]}{\mu bc}\dot{\omega}_1 + (\omega_3^2 - \omega_2^2)\omega_1 = \frac{[I_2 - I_3 - \mu b^2]}{\mu bc}\omega_2\omega_3. \quad (30)$$

This equation indicates that for the case $\omega_3 > \omega_2$, Equation 29 will result in damping of ω_1 to zero producing a stable spin about the maximum moment of inertia axis. The control law would be easy to implement, requiring measurement of z and ω_1 only. The mass would oscillate about its equilibrium position with decreasing amplitudes since ω_1 would be damped. The control mass would return to its zero position when ω_1 equals zero and a simple spin is reached. For the case of an arbitrary tumbling spacecraft, the assumption $\omega_3 > \omega_2$ cannot

be made and Equation 29 does not provide a satisfactory control law for the general case. However, the result may be useful in designing a control system for a space station which has an artifical-g mode where the spacecraft has a large rate about one axis, say ω_3, and the control system is to damp out the small transverse rates ω_1 and ω_2.

Since a simple spin about the maximum moment of inertia axis is the minimum energy state of the system, it is evident that Equation 29 produces energy dissipation for this case. The second specialized case demonstrates that a movable mass control system may increase the energy of the system to the maximum energy state. The vehicle would then be in a simple spin about its minimum moment of inertia axis. For this case the control mass motion is to be along a line oriented parallel to and offset by some distance a from the X_1 axis and passing through the X_2 axis. For this configuration Equation 16 becomes

$$[I_3 + \mu(x^2 + a^2)]\dot{\omega}_3 + [I_2 - I_1 + \mu(x^2 - a^2)]\omega_1\omega_2 + 2\mu x\dot{x}\omega_3 + \mu a x(\omega_2^2 - \omega_1^2) - \mu a\ddot{x} = 0. \quad (31)$$

Suppose the control law is now chosen to be

$$x = c\omega_3. \quad (32)$$

With this choice of control law and the assumption $I_2 >> \mu c^2\omega_3^2$, Equation 31 becomes

$$\ddot{\omega}_3 - \frac{[I_3 + \mu a^2]}{\mu ac}\dot{\omega}_3 + (\omega_1^2 - \omega_2^2)\omega_3$$

$$= \frac{[I_2 - I_1 + \mu a^2]}{\mu ac}\omega_1\omega_2. \qquad (33)$$

This equation indicates that if the product ac is chosen such that $ac < 0$, for the special case $\omega_1 > \omega_2$ Equation 32 will result in damping of ω_3 to zero and produce a simple spin about the minimum moment of inertia axis, X_1. The properties of the control law are similar to those of Equation 29.

The two preceding examples have demonstrated that the movable mass control system may increase or decrease the energy of the system and produce a simple spin about either the minimum or maximum moment of inertia axis for certain specialized cases. They also indicate that possibly the proper orientation for the direction of motion of the control mass is parallel to the desired final spin axis. However, since the initial tumble state of the vehicle is not known, the necessary assumptions may not be made for the general case of tumbling. The control laws given by Equations 29 and 32 are therefore attractive but inadequate in their simplicity. The formulation of a control law which will produce a simple spin for an arbitrary tumble state is the subject of the remainder of this section. Although the movable mass control system could possibly force a simple spin about

the minimum moment of inertia axis, the control law will be developed to produce spin about the maximum moment of inertia axis. Spin about this axis is stable in the presence of perturbing forces.

The development of the control law starts with the theory of Liapunov stability. From LaSalle (9), the system of differential equation given by Equations 14-16 and the mass equation of motion produced by the control law will be completely stable and approach its minimum state if there exists a scalar function V(u) with certain properties. The variable u is the state vector of the system. The conditions which the Liapunov function must satisfy are

a) $V(u) > 0$ for all $u \neq 0$

b) $\dot{V}(u) \leq 0$ for all u

c) $V(u) \to \infty$ as $\|u\| \to \infty$

where $\|u\|$ is the Euclidean norm of the state vector. For the physical system considered here, a convenient scalar function to use as a Liapunov function is the rotational kinetic energy of the system. Due to the nature of kinetic energy, conditions (a) and (c) will be automatically satisfied. Thus, if a control law is chosen such that condition (b) is satisfied, the system will be completely stable and approach its minimum state.

Consider the case where the control mass is restricted to move along a track parallel to the X_3 axis, and offset from this axis as shown in Figure 3. For this case, the rate of change of rotational kinetic energy given by Equation 27 simplifies to

$$\dot{T}_{rot} = \dot{z}f_3. \tag{34}$$

Thus, if the force applied to the control mass is selected as

$$f_3 = -\mu c\dot{z} \tag{35}$$

Equation 34 becomes

$$\dot{T}_{rot} = -\mu c\dot{z}^2 \tag{36}$$

which satisfies condition (b). Using Equations 19 and 35, the resulting equation of motion for the mass is

$$\ddot{z} + c\dot{z} - (\omega_1^2 + \omega_2^2)z = a\dot{\omega}_2 - b\dot{\omega}_1 - a\omega_3\omega_1 - b\omega_2\omega_3. \tag{37}$$

This equation has been written in a form which suggests that the mass dynamics are those of a second order system being forced by the motions of the tumbling vehicle. It should be noted, however, that the vehicle motions which produce the forcing function of Equation 37 are determined by differential equations which are themselves functions of control mass dynamics. If the effect of mass motion over one cycle is small, the dynamics of the

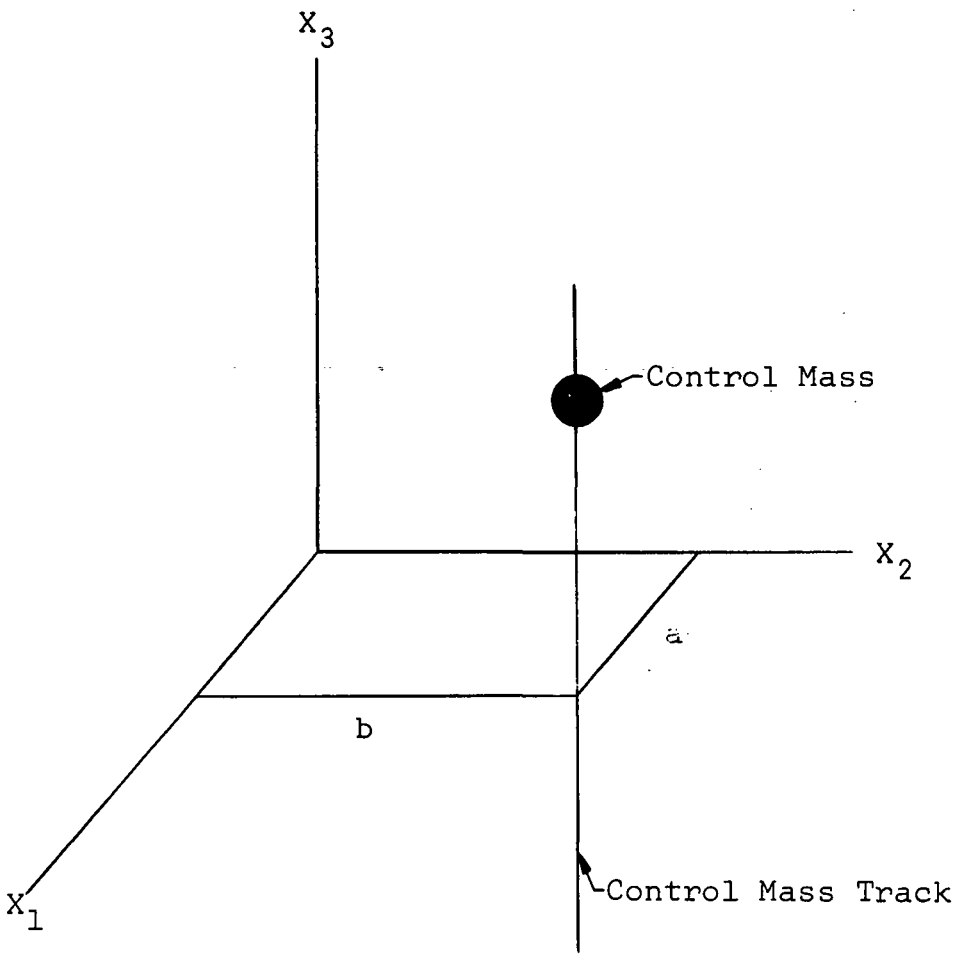

Figure 3. Orientation of Control Mass Path

vehicle are essentially those of a free uncontrolled body. With this assumption the forcing function of Equation 37 may be considered to be dominated by vehicle motions over one cycle. This form of the mass equation of motion may then be used to determine the effect of the control law on mass dynamics.

The control law given by Equation 35 satisfies condition (b) and decreases the rotational kinetic energy of the system. Also, the forcing function vanishes when a final spin about the X_3 axis is established. However, due to the negative, decaying coefficient of the z term, the mass would not necessarily return to its initial position (z = 0). Therefore, it is desirable to modify the control law to ensure the return of the control mass to its zero position once a simple spin state has been reached. This would restore the full control capability of the control system should another tumbling situation arise.

If the force applied to the control mass is modified such that

$$f_3 = -\mu c_1 \dot{z} - \mu(c_2 + \omega_1^2 + \omega_2^2) \tag{38}$$

the equation of motion for the mass becomes

$$\ddot{z} + c_1\dot{z} + c_2 z = a\dot{\omega}_2 - b\dot{\omega}_1 - a\omega_3\omega_1 - b\omega_2\omega_3. \tag{39}$$

The control law has been modified to cancel the undesirable negative coefficient of the z term and to provide a positive coefficient. With this control law, the mass equation of motion becomes a conventional second order differential equation which will provide damped motion of the mass and return the control mass to its zero position once a simple spin state is established.

The rate of change of rotational kinetic energy for this selection of control law is

$$\dot{T}_{rot} = -\mu c_1 \dot{z}^2 - \mu z \dot{z}(c_2 + \omega_1^2 + \omega_2^2). \qquad (40)$$

Here the formulation departs from the Liapunov method since $\dot{T}_{rot}$ is not necessarily negative semi-definite. The first term will decrease the rotational kinetic energy of the system while the second term will be oscillatory in nature, increasing and decreasing the energy. If the control system constants c_1 and c_2 are chosen properly the secular negative semi-definite term will dominate over the complete mass cycle. If every mass cycle has a net negative value for $\dot{T}_{rot}$, the system will approach its minimum energy state and a simple spin about the maximum moment of inertia axis. From the mass equation of motion, the mass would return to its zero position once this state has been reached. The physical significance of the control law given by Equation 38 will be discussed in Chapter IV.

Selection of Control System Parameters

For the selected control law, the rate of change of rotational kinetic energy is given by Equation 40 as a function of two control system parameters, c_1 and c_2. The parameter values should be chosen to yield a large value of energy dissipation rate and, hence, a fast approach to simple spin, subject to mass amplitude and power limitations. It is the purpose of this section to develop some guidelines for the selection of these parameter values.

Before proceeding with this development some qualitative observations will be made concerning the effect of c_1 and c_2 on control system performance. The right hand side of Equation 39 is again considered as the forcing function of mass dynamics so that

$$\ddot{z} + c_1\dot{z} + c_2 z = F \tag{41}$$

where the forcing function due to vehicle motion is

$$F = a\dot{\omega}_2 - b\dot{\omega}_1 - a\omega_3\omega_1 - b\omega_2\omega_3 \tag{42}$$

To investigate the effect of c_1 and c_2 on control system performance, an analogy is established between mass dynamics and a simple spring-mass-damper system. In this analogy, c_1 corresponds to the damping constant of the damper and c_2 corresponds to the spring constant of the spring.

Considering the expression for $\dot{T}_{rot}$ only, it may appear that the value of c_1 should be selected to be large since the negative semi-definite term is proportional to c_1. However this term is also a function of the relative velocity of the control mass so that the effect of a large value of c_1 on mass dynamics must be investigated. Referring to the spring-mass-damper analogy, a large value of c_1 corresponds to a strong damper which would limit the velocity of the mass. Since the negative semi-definite term of $\dot{T}_{rot}$ is the product of c_1 and the relative mass velocity squared, an increase in c_1 may result in a net decrease in the magnitude of this term. The proper value of c_1 must be determined considering both the direct effect of this parameter on $\dot{T}_{rot}$ and the indirect effect on the mass dynamics. A similar tradeoff results when the parameter c_2 is considered. The second term of $\dot{T}_{rot}$ is oscillatory in nature and results in energy addition over part of the mass cycle. This term is necessary to ensure the return of the control mass to its zero position once a simple spin state is reached. To limit the magnitude of the energy addition portion of the mass cycle, it may appear, from Equation 40, that c_2 should be selected to be a small value. However, again considering the spring-mass-damper analogy, a small

value of c_2 corresponds to a weak spring which would allow a relatively large amplitude of mass oscillation. These general considerations suggest that an optimum set of control system parameters may exist which maximize the energy dissipate rate while limiting the mass amplitude to a specified value. The remainder of this section presents some quantitative guidelines to aid in the selection of these parameter values.

An analytic solution of the mass equation of motion would provide control mass position and velocity histories as functions of the parameters c_1 and c_2. Using these solutions, the rate of change of rotational kinetic energy could be maximized subject to the condition of a selected maximum mass amplitude. This optimization could be performed using a Lagrange multiplier technique. Clearly, this is not possible since the forcing function, F, contains angular rates and accelerations of the vehicle. The solution of the mass equation of motion would therefore require the simultaneous solution of the vehicle equations of motion. This system of differential equations does not readily lend itself to an analytic solution due to the coupling and nonlinearities of these equations. On the other hand, a completely numerical solution of the system of equations provides no analytic information concerning the effect of the control system parameters. Therefore, a partially

analytical, partially numerical method was developed to provide some insight into the effect of the parameters on the performance of the control system.

The approach adopted is based on the assumption that the net change in the rotational kinetic energy over one mass cycle is small. With this assumption, the dynamics of the system are approximately those of a free, uncontrolled vehicle over one cycle. For a selected tumbling state, the free dynamics may be solved numerically. From results of the uncontrolled case, the forcing function of control mass dynamics, F, may be constructed using Equation 42. Although F will change as the control system reduces the tumbling, the initial tumble state will provide a design point which may be used to size control system parameters.

The nature of the forcing function may be investigated by considering the analytic solution of the free vehicle dynamics. From Synge and Griffith (10), the angular rates of a free asymmetric body may be expressed in terms of Jacobian elliptic functions. The result is

$$\omega_1 = \gamma \, cn \, [p(t - t_0)]$$

$$\omega_2 = \beta \, sn \, [p(t - t_0)] \qquad (43)$$

$$\omega_3 = \alpha \, dn \, [p(t - t_0)]$$

for the condition $H^2 > 2I_2T$ which corresponds to motion about the maximum moment of inertia axis, X_3. For the condition $H^2 < 2I_2T$, which corresponds to motion about the minimum moment of inertia axis, X_1, the solution is

$$\begin{aligned} \omega_1 &= \gamma' \, dn\,[p'(t - t_0)] \\ \omega_2 &= \beta' \, sn\,[p'(t - t_0)] \\ \omega_3 &= \alpha' \, cn\,[p'(t - t_0)]. \end{aligned} \tag{44}$$

The amplitudes, α, β, and γ, and the precession frequency, p, for the case $H^2 > 2I_2T$ and the corresponding quantities for the case of $H^2 < 2I_2T$ may be found in Synge and Griffith (10). The expressions for these quantities are not of direct concern here since it is only the form of the forcing function which is being investigated. Using these elliptic solutions, the forcing function will be in one of the following forms:

$$\begin{aligned} F = {} & a(p\beta - \alpha\gamma)cn[p(t - t_0)]dn[p(t - t_0)] \\ & + b(p\gamma - \alpha\beta)sn[p(t - t_0)]dn[p(t - t_0)] \end{aligned} \tag{45}$$

for $H^2 > 2I_2T$, and

$$\begin{aligned} F = {} & a(p'\beta' - \alpha'\gamma')cn[p'(t - t_0)]dn[p'(t - t_0)] \\ & + b(p'\gamma'k^2 - \alpha'\beta')sn[p'(t - t_0)]cn[p'(t - t_0)] \end{aligned} \tag{46}$$

for $H^2 < 2I_2T$.

The parameter k is the modulus of the elliptic functions. The functions sn u and cn u oscillate between 1 and -1 at the precession frequency p. The function dn u oscillates between 1 and $(1 - k^2)^{\frac{1}{2}}$ at twice the precession frequency.

From these considerations, it is evident that F will be oscillatory in form. Therefore, using the tabulated form of F obtained from the uncontrolled case results, a Fourier series may be fit to the data points. The forcing function expressed as a Fourier series will provide an analytical expression which can be used to solve the mass equation of motion. This solution will provide information concerning the relationship between control parameters and system performance.

The forcing function of the mass equation of motion expressed as a Fourier series is

$$F = A_0 + \sum_{n=1}^{\infty} \left(A_n \cos \frac{2n\pi t}{\tau} + B_n \sin \frac{2n\pi t}{\tau}\right)$$

where τ is the period of the function F. Since the forcing function, expressed as either Equation 45 or 46, contains no secular terms, $A_0 = 0$. Also, since F is a smooth function, the Fourier series may be terminated with a finite number term with sufficient accuracy. The Fourier expansion of the forcing function then becomes

$$F = \sum_{n=1}^{m} \left(A_n \cos \frac{2n\pi t}{\tau} + B_n \sin \frac{2n\pi t}{\tau}\right).$$

The Fourier coefficients, A_n and B_n, are determined numerically using a standard routine which generates Fourier coefficients for a tabulated function.

The Fourier expansion may be rewritten as

$$F = \sum_{n=1}^{m} D_n \sin \left(s_n t + \tan^{-1} \frac{A_n}{B_n}\right)$$

where

$$D_n = \sqrt{A_n^2 + B_n^2}$$

and

$$s_n = \frac{2n\pi}{\tau}.$$

The equation of motion of the mass then becomes

$$\ddot{z} + c_1\dot{z} + c_2 z = \sum_{n=1}^{m} D_n \sin \left(s_n t + \tan^{-1} \frac{A_n}{B_n}\right).$$

The particular solution of this equation may be readily obtained as

$$z_p = \sum_{n=1}^{m} E_n \sin \phi_n \tag{47}$$

where

$$E_n = \frac{D_n}{\sqrt{(c_2 - s_n^2) + (c_1 s_n)^2}}$$

and

$$\phi_n = s_n t + \tan^{-1} \frac{A_n}{B_n} - \tan^{-1} \frac{c_1 s_n}{c_2 - s_n^2}.$$

Differentiation yields the control mass velocity as

$$\dot{z}_p = \sum_{n=1}^{m} E_n s_n \cos \phi_n .$$

These solutions for control mass position and velocity histories may be used to determine the rate of change of rotational kinetic energy. The result is

$$\dot{T}_{rot} = -\mu \sum_{j=1}^{m} \sum_{k=1}^{m} [E_j E_k s_k \{c_1 s_j \cos \phi_j \cos \phi_k + (c_2 + \omega_1^2 + \omega_2^2) \sin \phi_j \cos \phi_k\}]. \quad (48)$$

Noting that

$$\cos \phi_j \cos \phi_k = \tfrac{1}{2}[\cos(\phi_j - \phi_k) + \cos(\phi_j + \phi_k)]$$

$$\sin \phi_j \cos \phi_k = \tfrac{1}{2}[\sin(\phi_j + \phi_k) + \sin(\phi_j - \phi_k)]$$

the secular part of Equation 48 may be identified as the terms for which j = k. Thus, the secular part of the rate of change of the rotational kinetic energy may be written as,

$$\dot{T}_{sec} = -\frac{\mu}{2} \sum_{n=1}^{m} c_1 E_n^2 s_n^2 .$$

Rewriting this equation to show the dependence of the control system parameters yields

$$\dot{T}_{sec} = -\frac{\mu}{2} \sum_{n=1}^{m} \frac{c_1 (A_n^2 + B_n^2) s_n^2}{[(c_2 - s_n^2)^2 + (c_1 s_n)^2]} \quad (49)$$

which may be used to determine the effect of control system variables on the secular part of the energy dissipation rate. This equation indicates that an increase in the weight of the control mass, and hence an increase in the reduced mass, μ, will linearly effect $\dot{T}_{sec}$. Increasing the Fourier coefficients A_n and B_n will increase $\dot{T}_{sec}$ quadradically. This may be accomplished by increasing the amplitude of the forcing function which corresponds to increasing the mass offset distances a and b. Thus, the control mass track should be placed at the maximum allowable distance from the center of mass of the vehicle.

The effect of c_1 and c_2 is more difficult to obtain but it is evident that c_2 should be of the order of s_n^2. With this assumption Equation 49 becomes

$$\dot{T}_{sec} \simeq -\frac{\mu}{2c_1} \sum_{n=1}^{m} (A_n^2 + B_n^2) \tag{50}$$

and Equation 47 becomes

$$z_p \simeq \frac{1}{c_1} \sum_{n=1}^{m} \frac{A_n^2 + B_n^2}{s_n} \sin \phi_n. \tag{51}$$

Equation 50 indicates that c_1 should be selected to be a small value. However, from Equation 51 decreasing c_1 results in increasing the maximum amplitude of the mass motion. These observations agree with the conclusions

drawn when the spring-mass-damper analogy was discussed. It can therefore be concluded that c_1 should be the smallest value which limits control mass amplitude to its maximum allowable value.

Equations 47 and 49 may be used to generate a nomograph for selection of control system parameters, c_1 and c_2. Once the control mass weight, track position, and an estimate of initial tumble state are obtained, $\dot{T}_{sec}$ may be calculated for various values of c_1 and c_2. Using Equation 47 the corresponding maximum mass amplitudes may be determined. Figure 4 shows a typical nomograph which will result. This particular nomograph was generated for an example case which will be discussed in Chapter IV. The figure shows a family of curves for $\dot{T}_{sec}$ as a function of the control system parameters c_1 and c_2. Also shown in the nomograph is another family of curves which connect sets of c_1 and c_2 values which result in a particular mass amplitude. As shown in Figure 4, each selected maximum mass amplitude has an associated optimum set of c_1 and c_2 values which corresponds to a maximum energy dissipation rate. Thus, once the maximum allowable mass amplitude has been determined the proper values of c_1 and c_2 may be selected from the generated nomograph.

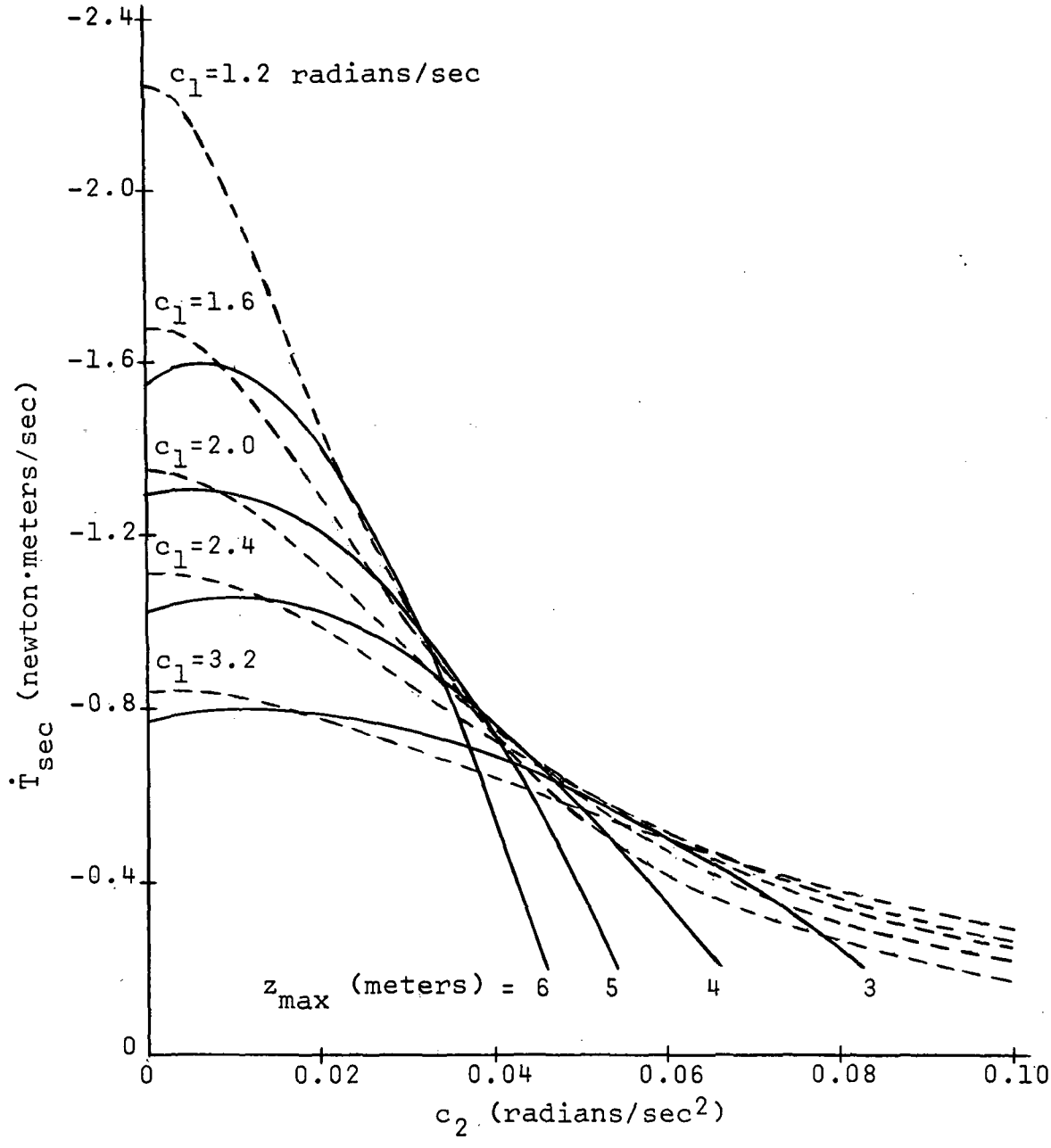

Figure 4. Control System Parameter Nomograph

The control system parameter selection procedure is simplified if the main vehicle is axially symmetric. For a symmetric vehicle the modulus of the elliptic functions, k, is zero and the Jacobian elliptic functions may be replaced with trigonometric functions. For this case

$$\text{sn}\,[p(t - t_0)] = \sin p(t - t_0)$$

$$\text{cn}\,[p(t - t_0)] = \cos p(t - t_0)$$

$$\text{dn}\,[p(t - t_0)] = 1.$$

The forcing function of mass dynamics then becomes

$$F = a(p\beta - \alpha\gamma)\cos p(t - t_0) + b(p\gamma - \alpha\beta) \sin p(t - t_0)$$

or

$$F = D \sin(pt + \delta)$$

where

$$D = \sqrt{a^2(p\beta - \alpha\gamma)^2 + b^2(p\gamma - \alpha\beta)^2}$$

$$\delta = \tan^{-1} \frac{a(p\beta - \alpha\gamma)}{b(p\gamma - \alpha\beta)} - pt_0.$$

The equation of motion of the mass may then be written as

$$\ddot{z} + c_1\dot{z} + c_2 z = D \sin(pt + \delta).$$

The particular solution of the mass equation of motion is then obtained as

$$z_p = \frac{D}{\sqrt{(c_2 - p^2)^2 + (c_1 p)^2}} \sin (pt + \delta - \tan^{-1} \frac{c_1 p}{c_2 - p^2}). \quad (52)$$

By noting the similarity between Equations 47 and 52, the secular part of the rate of change of rotational kinetic energy may be determined immediately from Equation 49 by setting $m = 1$ and $s_n = p$. Performing this yields

$$\dot{T}_{sec} = -\frac{\mu}{2} \frac{c_1 D^2 p^2}{[(c_2 - p^2)^2 + (c_1 p)^2]}. \quad (53)$$

The maximum mass amplitude may be readily obtained from Equation 52 as

$$z_{max} = \frac{D}{\sqrt{(c_2 - p^2)^2 + (c_1 p)^2}}. \quad (54)$$

The values of c_1 and c_2 which yield the maximum energy dissipation rate with the side condition of a selected maximum mass amplitude may be determined using a Lagrange multiplier technique.

Before proceeding with this formulation, Equation 41 will be written in standard second order form as

$$\ddot{z} + 2\zeta\omega_n\dot{z} + \omega_n{}^2 z = F$$

where ζ is the damping ratio and ω_n is the natural frequency of the system. Comparing this standard form with Equation 41 the following relations are evident.

$$c_1 = 2\zeta\omega_n$$

$$c_2 = \omega_n{}^2$$

Applying these relations to Equation 53 and rearranging yields

$$\dot{T}_{sec} = -\frac{\mu D^2}{2p} \frac{\zeta(\frac{\omega_n}{p})}{(\frac{\omega_n}{p})^4 + 2(2\zeta^2 - 1)(\frac{\omega_n}{p})^2 + 1}.$$

Defining the parameter, $\nu \overset{\Delta}{=} \frac{\omega_n}{p}$, this equation becomes

$$\dot{T}_{sec} = -\frac{\mu D^2}{2p} \frac{\zeta\nu}{\nu^4 + 2(2\zeta^2 - 1)\nu^2 + 1}.$$

Similarly, the maximum mass amplitude becomes

$$z_{max} = \frac{D}{p^2} \frac{1}{\sqrt{\nu^4 + 2(2\zeta^2 - 1)\nu^2 + 1}}.$$

The maximum value of $\dot{T}_{sec}$ corresponding to a selected maximum mass amplitude is determined by constructing the function

$$G = -\frac{\mu D^2}{2p} \frac{\zeta\nu}{\nu^4 + 2(2\zeta^2 - 1)\nu^2 + 1}$$

$$+ \lambda\left[\frac{z_{max}p^2}{D}\sqrt{\nu^4 + 2(2\zeta^2 - 1)\nu^2 + 1}\right].$$

Taking the partial derivatives of G with respect to ζ, ν, and λ, setting these expressions equal to zero and solving the resulting system of equations yields the optimum values of ζ and ν. Performing these operations yields three values for ν.

$$\nu = 0, \quad \nu = \pm 1$$

Obviously, $\nu = 0$ corresponds to a minimum, since $\dot{T}_{sec} = 0$ for $\nu = 0$, and $\nu = -1$ corresponds to a maximum which results in an increase in rotational kinetic energy. The desired value as $\nu = 1$ which corresponds to

$$\omega_n = p$$

or

$$c_2 = p^2. \tag{55}$$

Thus, the natural frequency of the control system should be selected to equal the driving frequency of the forcing function for maximum energy dissipation. For $\nu = 1$, the maximum mass amplitude is

$$z_{max} = \frac{D}{2p^2\zeta}$$

and, hence,

$$\zeta = \frac{D}{2p^2 z_{max}} .$$

Thus, parameter c_1 should be chosen such that

$$c_1 = \frac{D}{pz_{max}} . \tag{56}$$

For these values of c_1 and c_2

$$\dot{T}_{sec} = -\frac{\mu D p z_{max}}{4} .$$

From this equation, the energy dissipation rate may be increased by increasing the control mass weight, moving the mass track away from the center of mass which increases D, or by allowing the mass a larger amplitude. These observations agree with the results obtained for the general case discussed previously. As can be seen the selection of control system parameters c_1 and c_2 is simplified for a symmetric vehicle. Once the initial tumble dynamics have been analyzed, the parameter values may be calculated directly using Equations 55 and 56 instead of generating a nomograph as was done for the general case.

Although the methods presented for the selection of control system parameters may be in error due to the assumptions and approximations made, the procedures outlined will provide "ballpark" estimates of c_1 and c_2

values. Final selection of c_1 and c_2 values must be based on the actual dynamics of the system obtained by solving the complete vehicle and mass equations of motion.

Sensor and Power Requirements

The sensor and power requirements of the movable mass control system with the selected control law will be discussed briefly in this section.

For the control law expressed as Equation 38 it is evident that the following quantities must be sensed: f_3, the force applied to the control mass; $\dot{z}$, the control mass velocity relative to the vehicle; z, the control mass position; and the combination $(\omega_1^2 + \omega_2^2)$. The quantity f_3 may be determined using a linear accelerometer mounted on the control mass. If the accelerometer is mounted to detect the $\hat{k}$-component of mass acceleration, the sensed acceleration will be proportional to f_3. The mass position and velocity may be easily sensed using any of a number of simple devices. The combination $(\omega_1^2 + \omega_2^2)$ may be determined with a linear accelerometer mounted on the X_3 axis. The acceleration of a fixed point, P, located by a vector $\vec{d}$ from the vehicle center of mass is

$$\vec{a}_P = \vec{\omega} \times (\vec{\omega} \times \vec{d}) + \dot{\vec{\omega}} \times \vec{d}$$

If $\vec{d} = d\hat{k}$ the $\hat{k}$-component of $\vec{a}_p$ is

$$(a_p)_3 = -d(\omega_1^2 + \omega_2^2).$$

Thus, an accelerometer placed at this point and oriented to sense the $\hat{k}$-component of the acceleration at that point will sense a quantity proportional to $(\omega_1^2 + \omega_2^2)$. The sensor requirements for the implementation of the control law appear to be modest.

The force requirements of the control system may be determined by Equation 19 since this is the force applied by the control system to the control mass. The instantaneous power required by the control system is, by definition, the force applied to the mass times the relative velocity. This definition is equivalent to Equation 27 which gives the rate of change of rotational kinetic energy of the system. As noted in the second section of this chapter $\dot{T}_{rot}$ will be oscillatory, the negative portions of $\dot{T}_{rot}$ resulting in energy dissipation. Thus, the power input to the mass corresponds to the positive portions of $\dot{T}_{rot}$. In fact, if a power generation system would be implemented with the control system, energy could be stored during the energy dissipation portions of the mass cycle and be used to power the positive $\dot{T}_{rot}$ portions of the cycle. This possibility is not considered further since the primary function of the control system is to aid in crew rescue and not generate power. For

this case, the energy input required is just the integral of the positive portions of the $\dot{T}_{rot}$ curve. The force, power, and energy requirements for two example cases will be discussed in the next section.

CHAPTER IV

RESULTS

To demonstrate the feasibility of a movable mass control system using the control law given by Equation 38, the space station shown in Figure 5 was chosen as an example vehicle. The geometric axes shown in Figure 5 are assumed to be the principal axes for demonstration purposes. The properties of this Modular Space Station (MSS) are given below.

$$I_1 = 5.15 \times 10^6 \text{ kg-m}^2 (3.80 \times 10^6 \text{ slug-ft}^2)$$

$$I_2 = 6.28 \times 10^6 \text{ kg-m}^2 (4.63 \times 10^6 \text{ slug-ft}^2)$$

$$I_3 = 6.74 \times 10^6 \text{ kg-m}^2 (4.97 \times 10^6 \text{ slug-ft}^2)$$

$$M = 9.98 \times 10^4 \text{ kg} (2.20 \times 10^5 \text{ lbm})$$

The space station shown in Figure 5 was selected since it is a relatively large vehicle and does not have an artificial-g mode. Thus, a passive damping system such as a viscous ring or pendulum damper would not be practical for this application.

The tumble state used for this example was obtained from Kaplan (11). The initial rates are

$$\omega_1(0) = -2.86 \times 10^{-4} \text{ radians/sec}$$

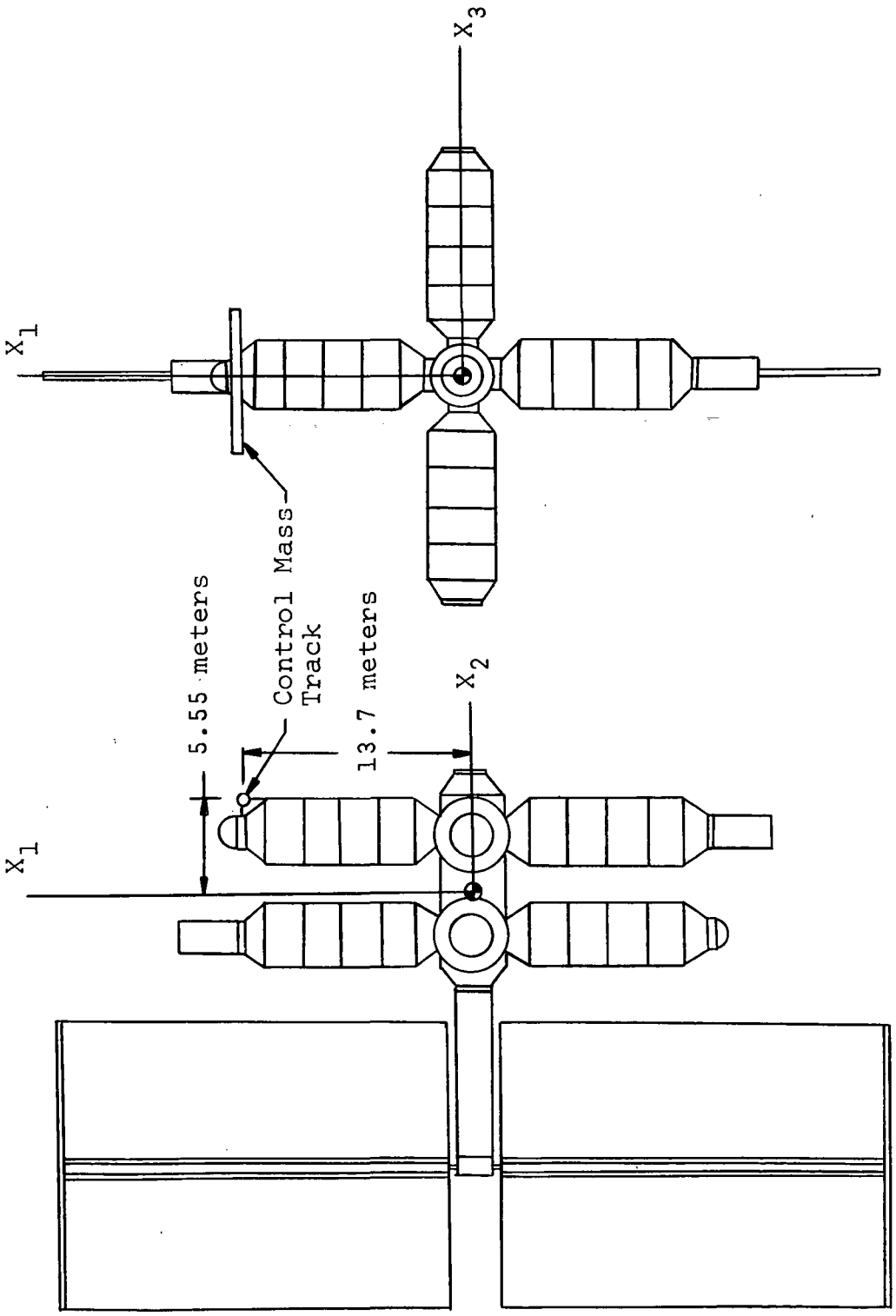

Figure 5. Modular Space Station Configuration

$$\omega_2(0) = -0.199 \text{ radians/sec}$$

$$\omega_3(0) = 0.103 \text{ radians/sec.}$$

These values are based on a realistic worst case analysis of the tumble state produced by a collision of a shuttle orbiter and the MSS. Since the resultant tumble state is dependent on the amount of kinetic energy transferred by the orbiter to the MSS, the initial tumble conditions are given by Kaplan for 10, 50, and 100 percent kinetic energy transfer. Although the 100 percent case corresponds to a perfectly elastic collision which would not be the case, it does produce the highest tumble rates and was, therefore, selected to test the movable mass control system.

For an uncontrolled vehicle, the selected initial conditions result in the tumble state shown in Figure 6. As can be seen, this tumble state is fairly severe and by no means lends itself to the assumption of small transverse rates since the amplitudes of the angular velocity oscillations are all of the same order of magnitude.

The control mass track is placed at the farthest allowable point from the vehicle center of mass and oriented parallel to the maximum moment of inertia axis as shown in Figure 5. For this positioning, the mass track offset distances are

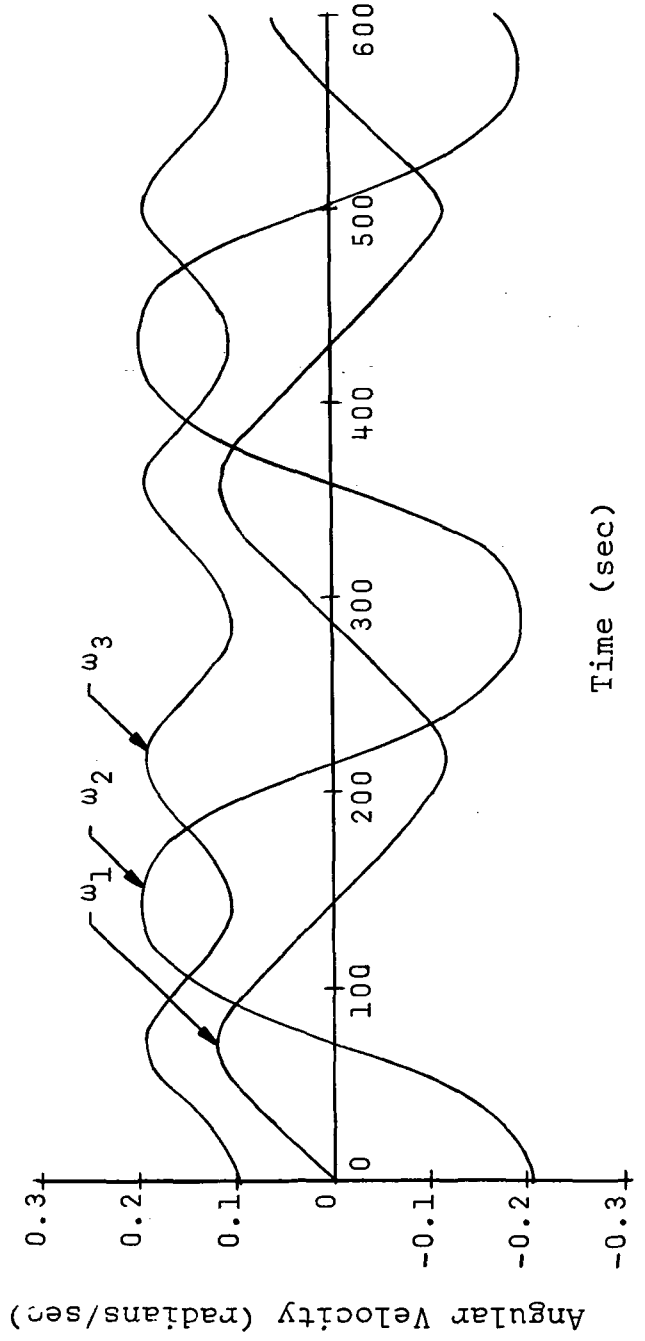

Figure 6. Uncontrolled Spacecraft Dynamics

a = 13.7 meters (45 feet)

b = 5.5 meters (18 feet).

For these offset distances and the uncontrolled dynamics shown in Figure 6 the forcing function of the mass equation of motion, given by Equation 42, may be constructed. The result is shown in Figure 7. It is interesting to note that, comparing Equations 19 and 42, F is the negative of the force on a unit mass attached to the tumbling vehicle with coordinates (a, b, 0). Thus, Figure 7 shows a typical acceleration profile that a crewman would experience inside the tumbling vehicle. As shown in Figure 7 the acceleration would be constantly changing magnitude and direction and would create an extremely hazardous environment for the crew. A simple spin, on the other hand, produces constant forces with constant directions which would greatly aid the crew in evacuation operations.

Using the forcing function shown in Figure 7, the coefficients of the Fourier series representing the forcing function were determined. Then, using Equations 47 and 49, the secular part of the rate of change of the rotational kinetic energy and the maximum mass amplitude were determined for various values of c_1 and c_2. The resulting nomograph was discussed in Chapter III and is shown in Figure 4. A control mass of 99.8 kg (200 lbm) which corresponds to 0.1 percent of the vehicle weight

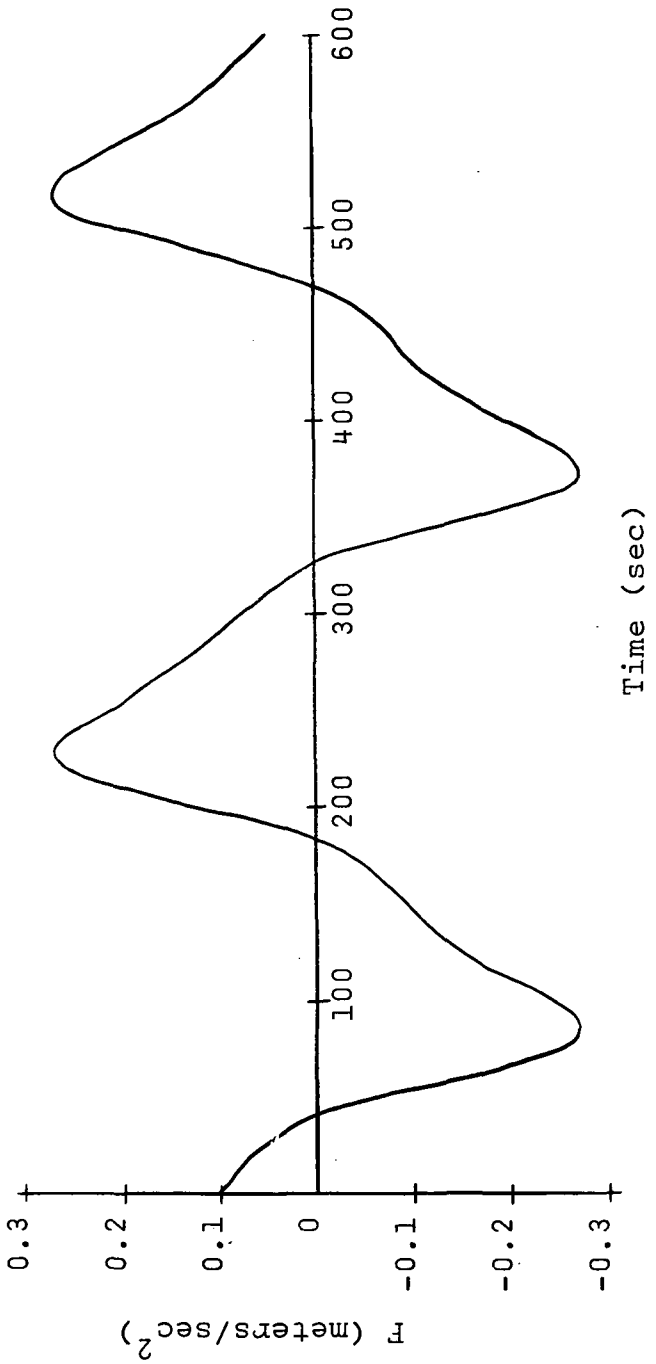

Figure 7. Mass Equation of Motion Forcing Function

was used to generate the nomograph. Different values of control mass weight will shift the curves up or down but will not affect the shape of the curves. The dotted lines on the nomograph gives the secular rate of change of rotational kinetic energy as a function of control system parameters c_1 and c_2. From Figure 4, smaller values of c_1 give larger values of $\dot{T}_{sec}$. Also shown on the nomograph by solid lines are points which result in the same maximum mass amplitude. For each selected maximum allowable mass amplitude there appears to be an optimum set of c_1 and c_2 which results in the optimum value of $\dot{T}_{sec}$. Thus, once the maximum mass amplitude has been determined, the proper control system parameters may be chosen using the nomograph. This nomograph is dependent on the initial tumble state selected as the design point.

Although the nomograph shows relatively large energy dissipation rates for $c_2 = 0$, the assumptions under which the nomograph was generated must be kept in mind. It was assumed that the forcing function would be purely oscillatory so that it could be approximated by a Fourier series. For the actual case, however, the forcing function will not be purely oscillatory, in general, since the system is being damped. A value of $c_2 = 0$ corresponds to having no spring in the spring-mass-damper analogy discussed previously. Therefore, the non-oscillatory nature

of the forcing function will cause the control mass oscillations to migrate away from its initial position for $c_2 = 0$. Thus, a non-zero value of c_2 is required to prevent this and insure the return of the control mass to its initial position.

Once the control system parameters have been selected, the mass and vehicle equations of motion may be solved. This was done using a fourth-order Runge-Kutta algorithm to numerically solve the system of differential equations with an IBM 370-165 computer. The accuracy of the algorithm was checked using the fact that the angular momentum of the system about the composite center of mass is constant in the absence of external moments.

Before stating the results, the physical significance of the control law given by Equation 38 will be discussed briefly. Figures 8a and 8b show typical cycles of control force acting on the control mass, f_3, and velocity relative to the body fixed axes, $\dot{z}$, respectively. Comparing Figures 8a and 8b it is evident that the control law causes the control force to be generally opposite to the relative velocity. Figure 8c shows the rate of change of rotational kinetic energy of the system which is the product of total force and relative velocity. It can be seen that $\dot{T}_{rot}$ is generally negative

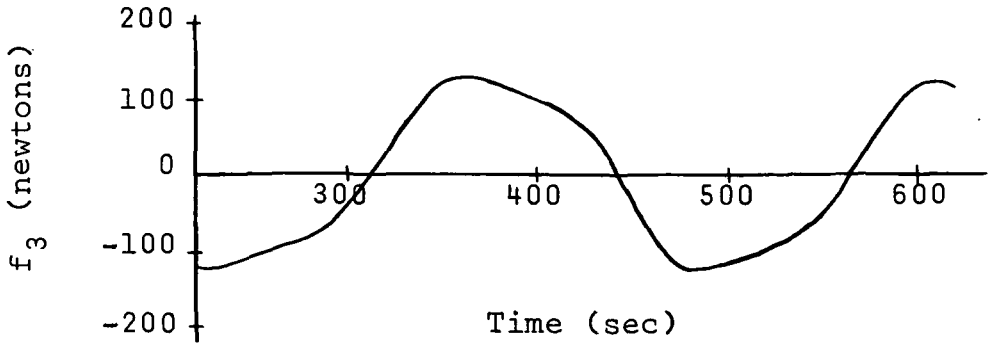

a) Control Force

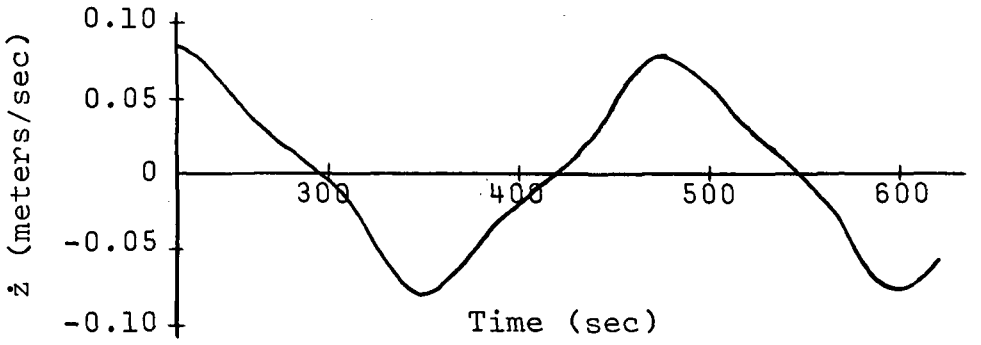

b) Mass Velocity

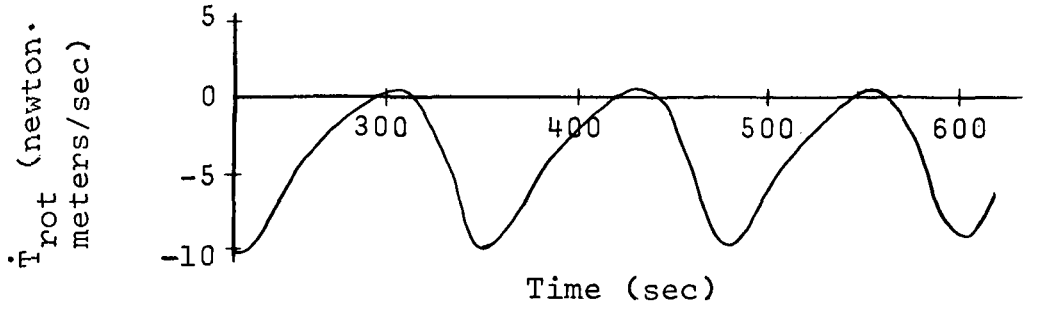

c) Energy Dissipation Rate

Figure 8. Typical Cycles of Control Force, Mass Velocity, and Energy Dissipation Rate

which corresponds to energy dissipation. The positive portions of $\dot{T}_{rot}$ correspond to energy addition. These portions are due to the second term of Equation 40 which was selected to insure that the control mass oscillates about its zero position and returns there after simple spin is established. In general, energy addition is not desired but from Figure 8c it can be seen that over a complete cycle there is a large energy dissipation and only a relatively small energy addition over each cycle. Therefore, it was determined that this energy addition was acceptable to insure return of the control mass to its zero position. The situation is further clarified by Figure 9 which shows typical cycles of control mass position over the same time period as the quantities shown in Figure 8. Superimposed on the mass cycle is a schematic of the control mass with the directions of the mass velocity and the force acting on the mass shown. It is evident that the force given by the control law is generally a retarding force. In the first half cycle the mass is moving "up" and the applied control force is directed "down" which produces energy dissipation. Eventually this force will overcome the velocity and the force and velocity will be in the same direction resulting in energy addition as shown in Figure 8c. This situation occurs only over a small part

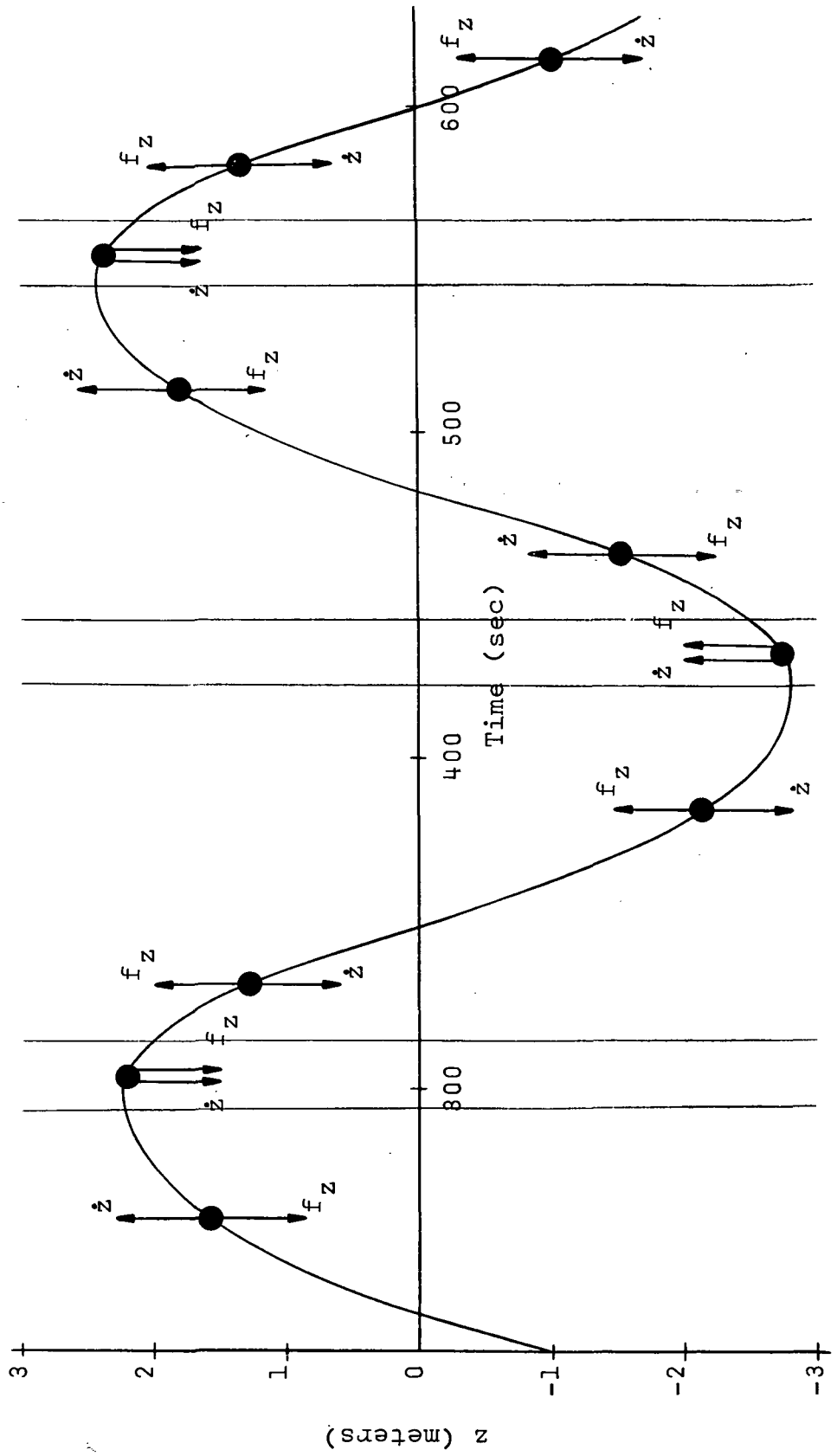

Figure 9. Typical Cycle of Control Mass Position

of the mass cycle, however. After this portion of the half cycle, the force and velocity will again be directed oppositely producing more energy dissipation. A similar process occurs during the second half cycle and produces a net decrease in the rotational kinetic energy of the system over the complete mass cycle. A net decrease in the energy over every mass cycle allows the system to approach its minimum energy state producing a simple spin about the maximum moment of inertia axis.

If a maximum mass amplitude of three meters is selected, the proper values of c_1 and c_2 are, from Figure 4

$$c_1 = 3.2 \text{ radians/sec}$$

$$c_2 = 0.02 \text{ radians/sec}^2.$$

For a control mass weight of 998 kg (2,200 lbm), the stated initial conditions, and the selected parameter values, the resultant angular velocity histories are shown in Figure 10. Since it is not the oscillations themselves but the decay of the oscillation amplitudes which is important, only the envelopes formed by the oscillations are shown in Figure 10. The control system effectively collapses the ω_1 and ω_2 envelopes to zero. As this is being done the mean value of the ω_3 oscillation increases to its steady spin value as it must do to keep the angular momentum of the system constant.

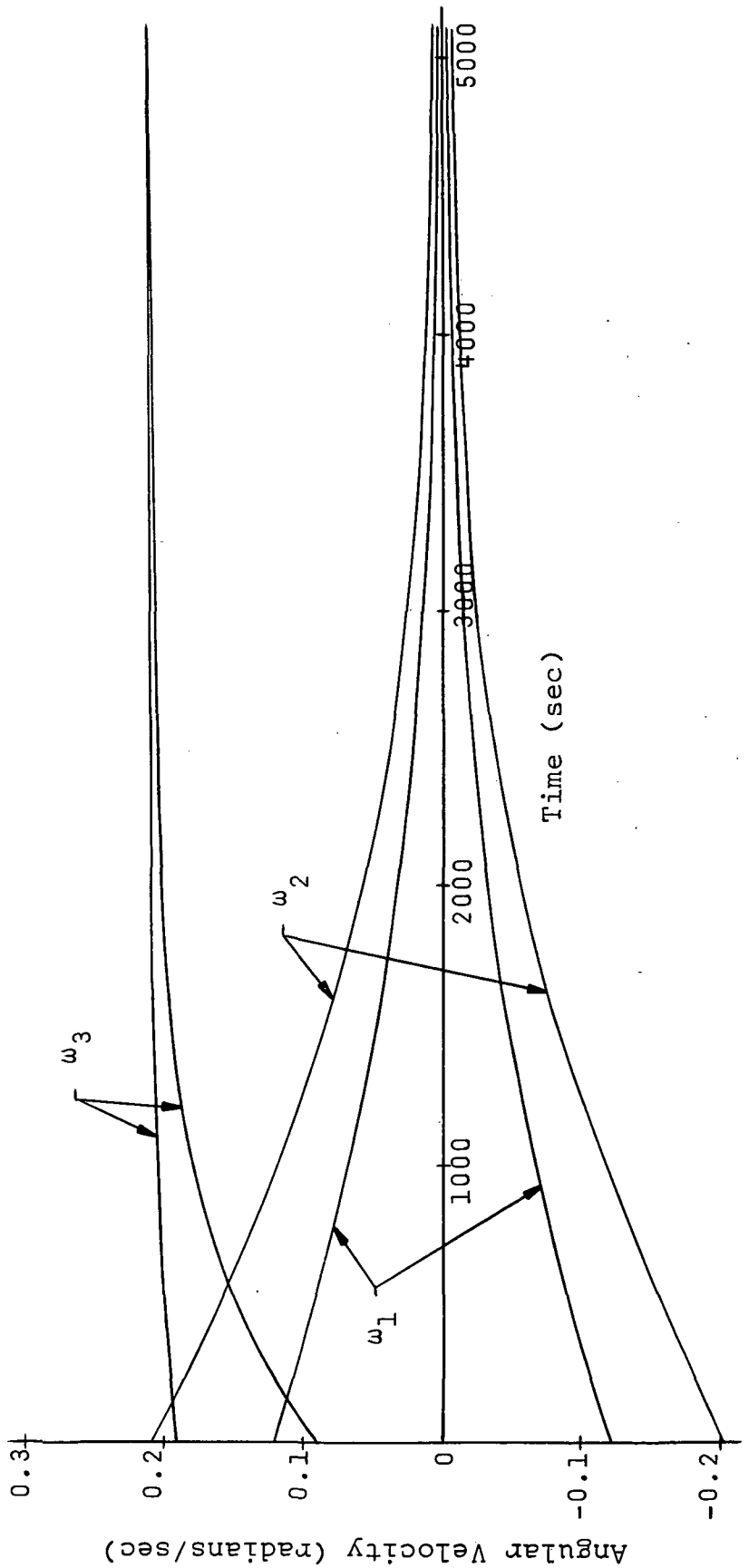

Figure 10. Envelopes of Angular Velocity Oscillations

Thus, the control system eliminates the transverse angular rates and produces a simple spin about the maximum moment of inertia axis.

Figure 11 shows the envelope formed by the control mass oscillations. Figure 11 indicates that the maximum mass amplitude exceeds the predicted value of three meters slightly. This may be attributed to the homogeneous solution of the mass equation of motion which was neglect in determining the nomograph shown in Figure 4. The results indicate that this overshoot occurs only during the first mass cycle and, since the overshoot is small, the neglect of the homogeneous solution is justified. It may also be noted that during the first part of the control period the mass oscillations are not symmetric about the zero position. This may also be attributed to the homogeneous solution since the oscillations become symmetric as the homogeneous solution decays. The homogeneous solution corresponds to the transient response of the control system.

Figure 12 shows the time history of the rotational kinetic energy of the system. The figure indicates that the rotational kinetic energy is oscillatory due to the slight energy addition during each cycle but due to the dominant energy dissipation portion of the mass cycle the system approaches its minimum energy state.

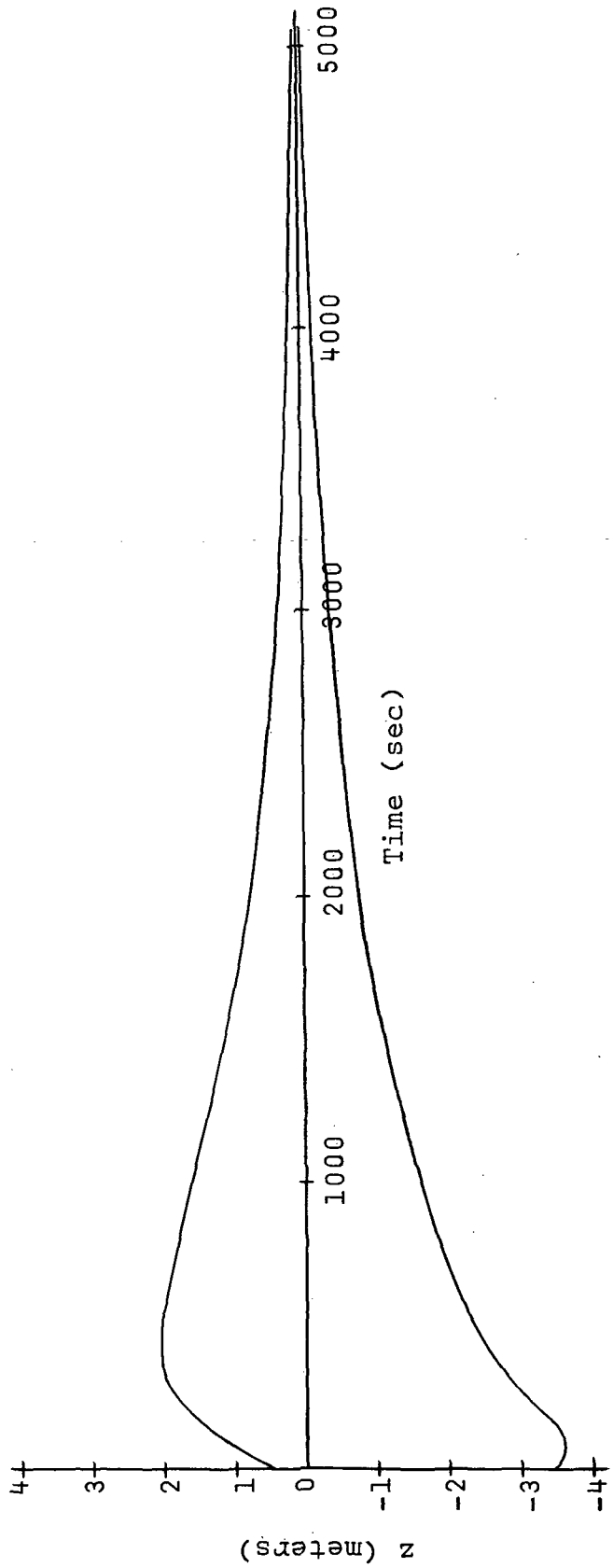

Figure 11. Envelope of Control Mass Oscillations

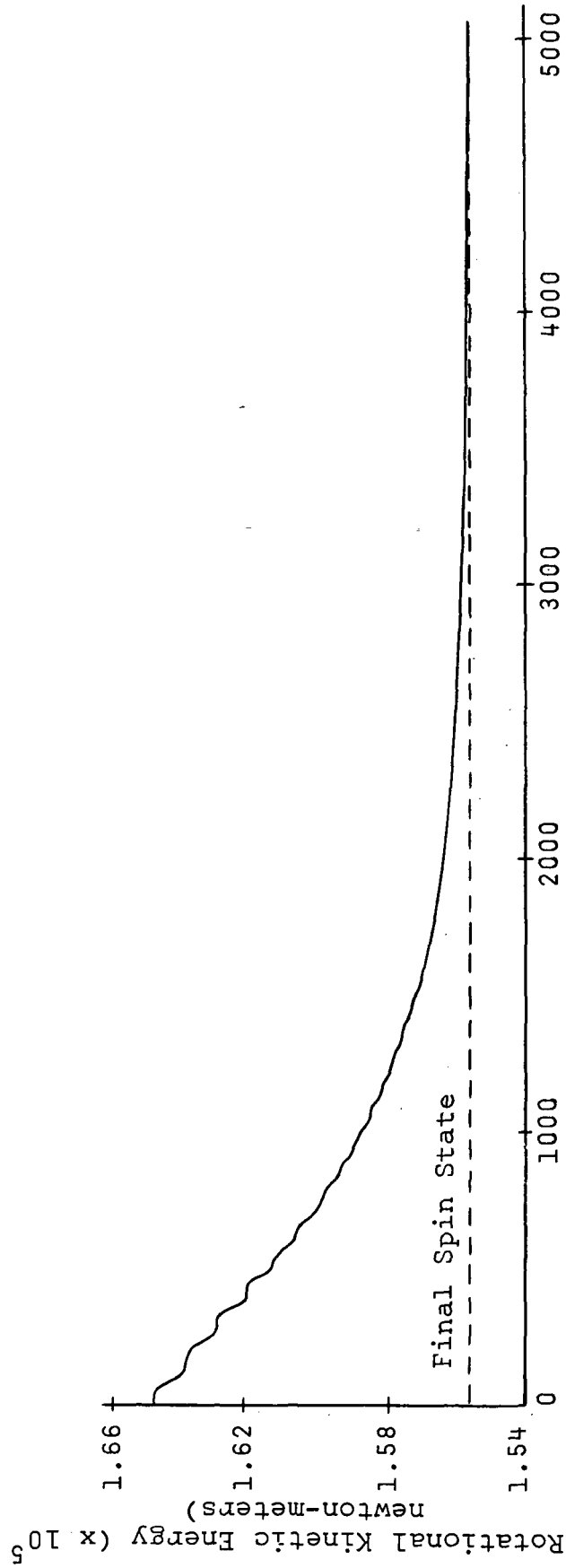

Figure 12. Time History of System Rotational Kinetic Energy

Figures 10, 11, and 12 indicate that for the stated initial conditions, a maximum mass amplitude of approximately three meters, and a control mass weight of 998 kg (2,200 lbm), a movable mass control system using the control law given by Equation 38 is capable of converting the tumbling motions of the MSS into simple spin within two hours. To investigate the effect of various parameters on control system performance a time constant will be defined. The time constant, τ_c, is defined as the time required for the control system to collapse the ω_1 or ω_2 oscillation envelope to a value of 1/e times its initial value. Since the general shape of the performance curves corresponding to other parameter values will be similar to those shown in Figures 10-12 this time constant will be used to compared control system performance for various cases.

The effect of control mass weight on system performance is shown in Figure 13. The figure shows that an increase in control mass weight has a marked effect on the system time constant. The shape of the curve is as expected since an extremely small mass produces very little energy dissipation while an extremely large mass produces a large energy dissipation rate and, hence, a small time constant. However, the peak power and force required also increases with increased control mass weight

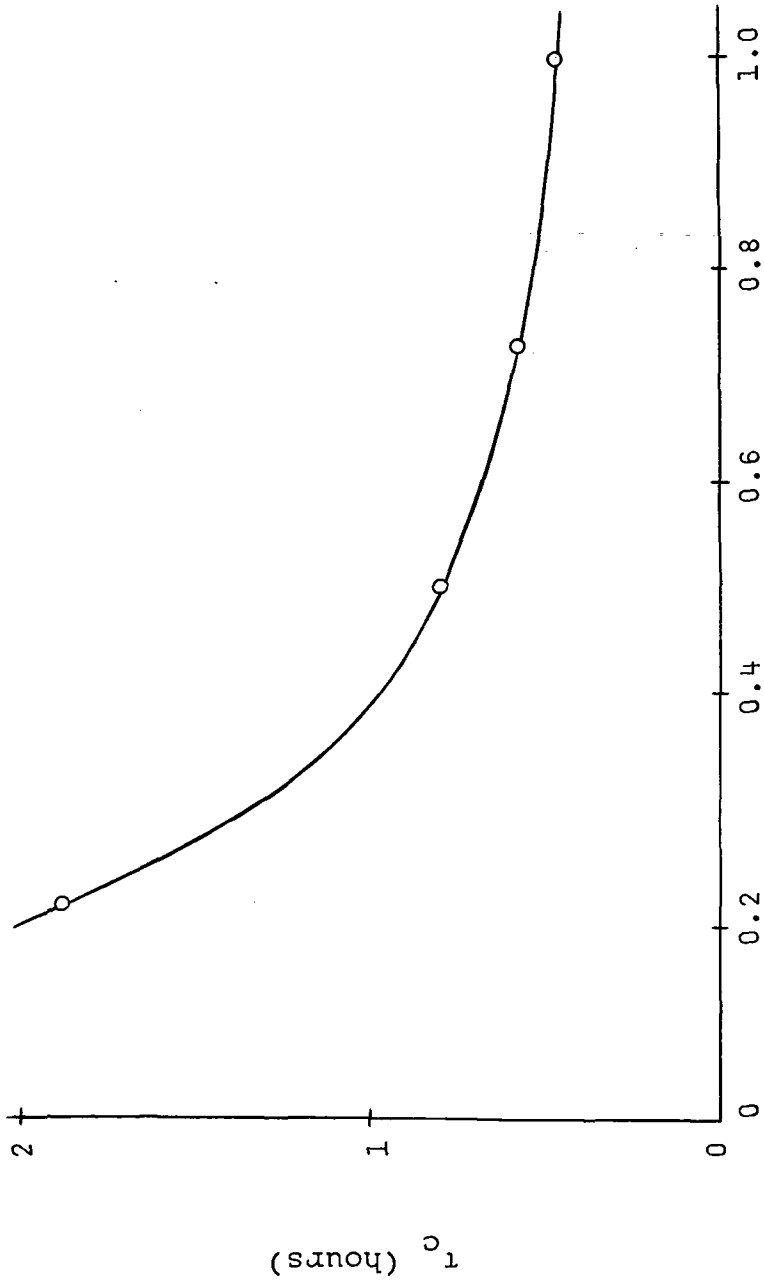

Figure 13. Variation of Time Constant with Control Mass Weight

as shown in Figures 14 and 15. Thus, the control mass weight should be selected as large as possible consistant with the imposed weight, power, and force limitations. Surprisingly, the total energy required to operate the control system does not vary appreciably with control mass weight. The energy requirements for the example considered here are shown in Table I for various control mass weights. Thus, for this case the control system seems to damp the system quickly, requiring high values of power and force, or damp the system slowly, requiring lower values of power and force, such that the total energy required is approximately constant.

All of the cases discussed so far have been for control system parameters of c_1 = 3.2 sec^{-1} and c_2 = 0.02 sec^{-2} and a corresponding maximum mass amplitude of 3.7 meters (12 feet). To demonstrate the effect of increased mass amplitude on control system performance two other sets of c_1 and c_2 values were selected from Figure 4. The result is shown in Figure 16 which gives the variation of the defined time constant, τ_c, with maximum mass amplitude for a control mass of 499.0 kg (1,100 lbm). Table II gives the values of c_1 and c_2 that were used along with the resulting maximum amplitudes during the first and second mass cycles and the predicted values given by Figure 4. As can be seen from the table,

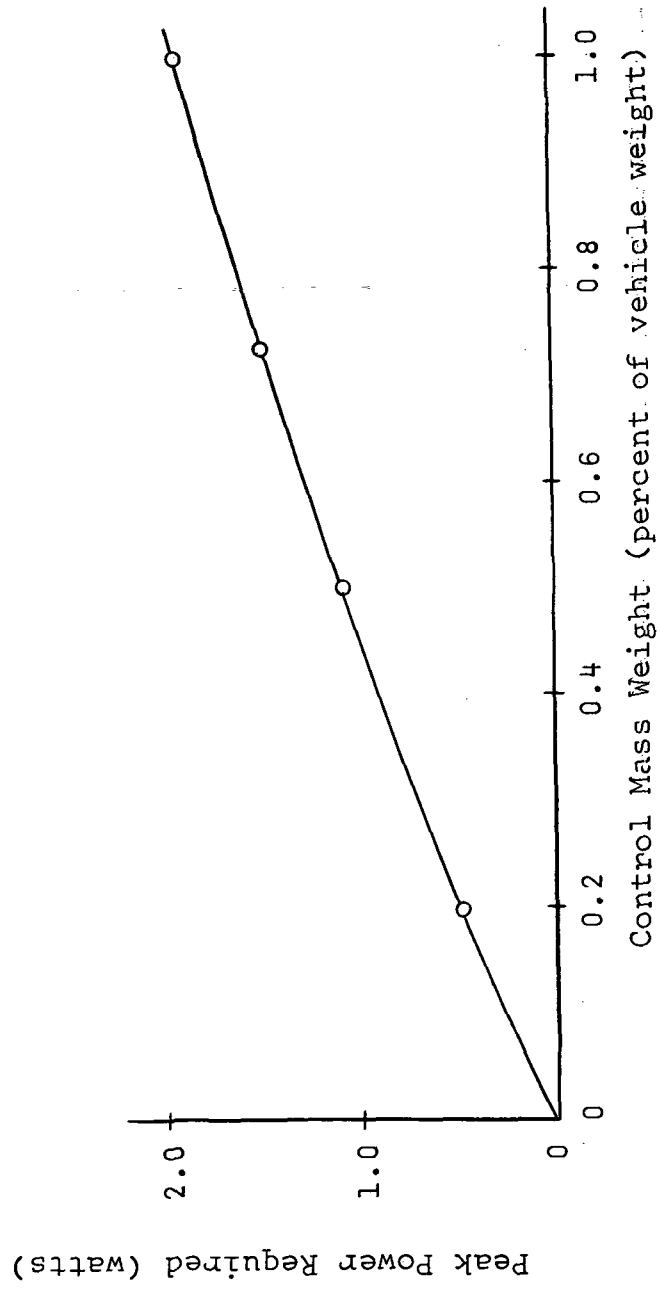

Figure 14. Variation of Peak Power with Control Mass Weight

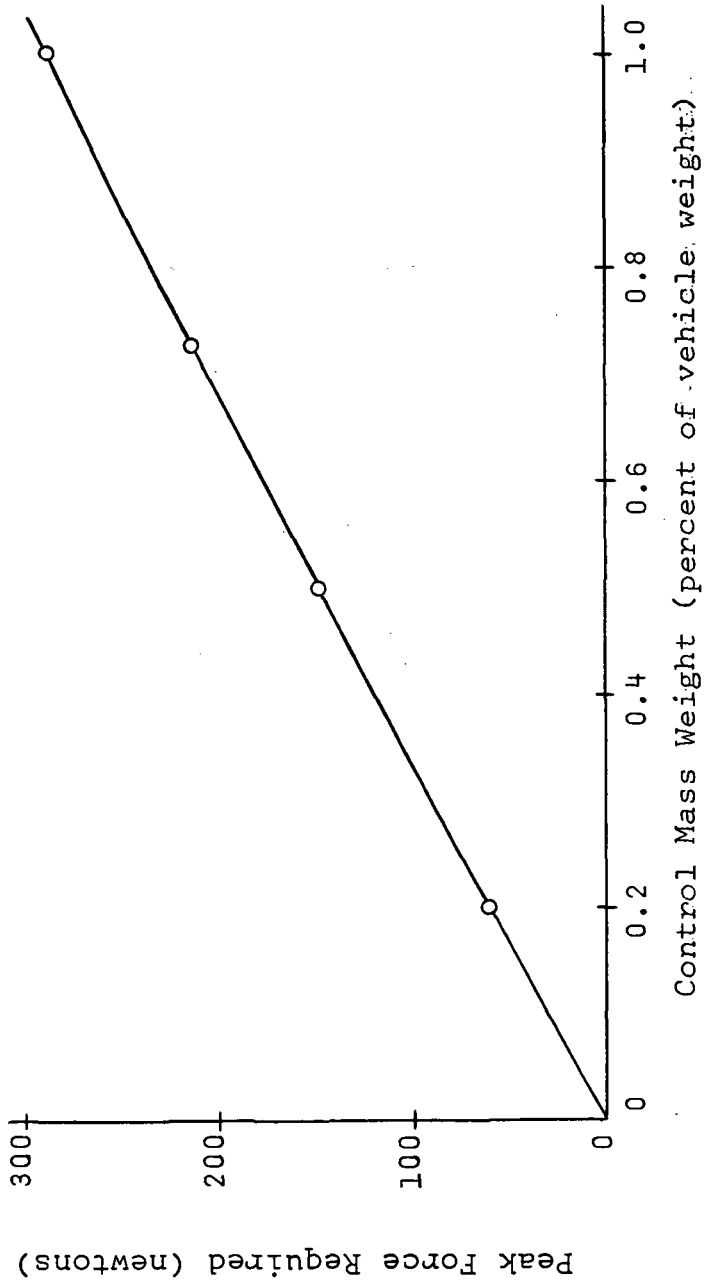

Figure 15. Variation of Peak Force Required with Control Mass Weight

Table I

Variation of Required Energy with Control Mass Weight

Control Mass Weight	Required Energy
199.6 kg (440 lbm)	63.9 watt-sec
499.0 kg (1,100 lbm)	68.7 watt-sec
725.8 kg (1,600 lbm)	71.6 watt-sec
998.0 kg (2,200 lbm)	74.6 watt-sec

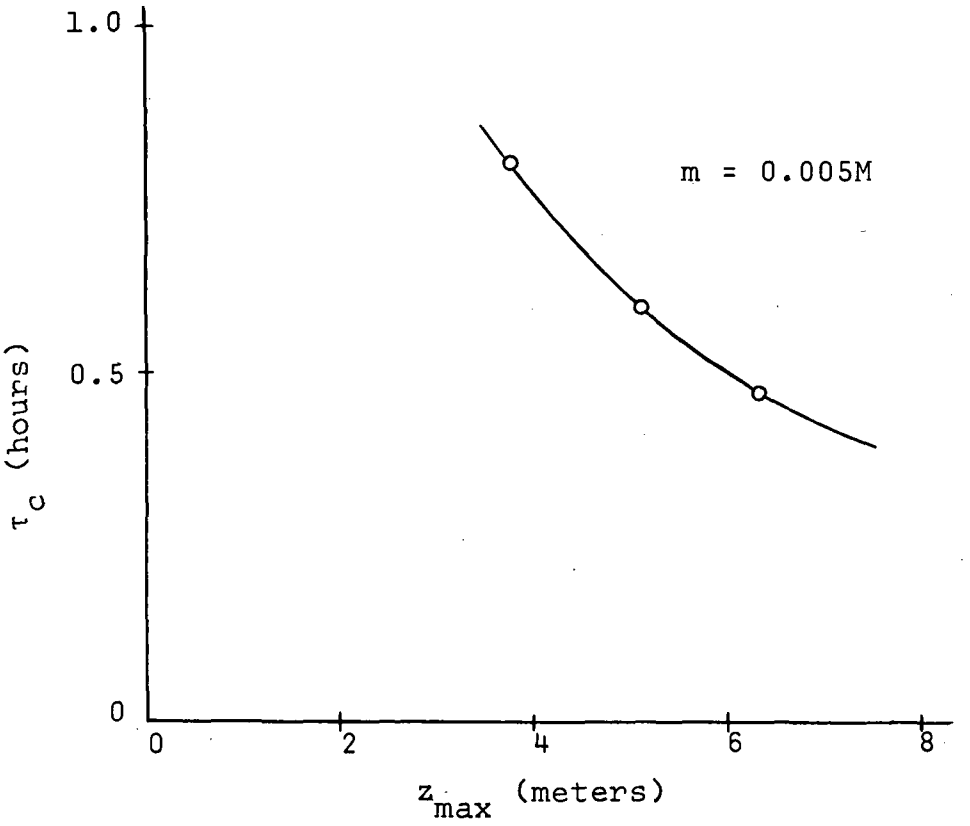

Figure 16. Variation of Time Constant with Maximum Mass Amplitude

Table II

Predicted and Actual Maximum Mass Amplitudes for Modular Space Station Simulation

c_1 (radians/sec)	c_2 (radians/sec^2)	Predicted z_{max} (meters)	Actual z_{max} (meters) First Cycle	Second Cycle
3.2	0.020	3.0	3.7	2.8
2.4	0.014	4.0	5.1	3.7
1.9	0.012	5.0	6.3	4.6

the predicted maximum amplitude falls between the actual maximum amplitudes during the first and second mass cycles. It may also be noted that the larger the mass amplitude the larger the overshoot relative to the predicted value indicating the increased effect of the homogeneous solution.

An additional application of a movable mass control system as a wobble damper was investigated. The example vehicle used is the NASA 21 Man Space Station which is a hexagonal shaped, spin stabilized, artificial gravity space vehicle shown in Figure 17. The properties of this vehicle are given below

$I_1 = I_2 = 1.42 \times 10^7$ kg-meter^2 (10.5×10^6 slug-ft^2)

$I_3 = 2.03 \times 10^7$ kg-meter^2 (15.0×10^6 slug-ft^2)

$M = 6.21 \times 10^4$ kg (1.37×10^5 lbm)

Nominal spin rate = 0.314 radians/sec (3 rpm)

This vehicle was the basis of a study by TRW Space Technology Laboratories (12) to investigate the feasibility of several passive damping devices for use as wobble dampers. The devices studied were a controlled damping pendulum, a viscous ring damper, a pendulum damper, and a Naval Ordinance Test Station (NOTS) mercury ring damper. Selection of this vehicle as an example

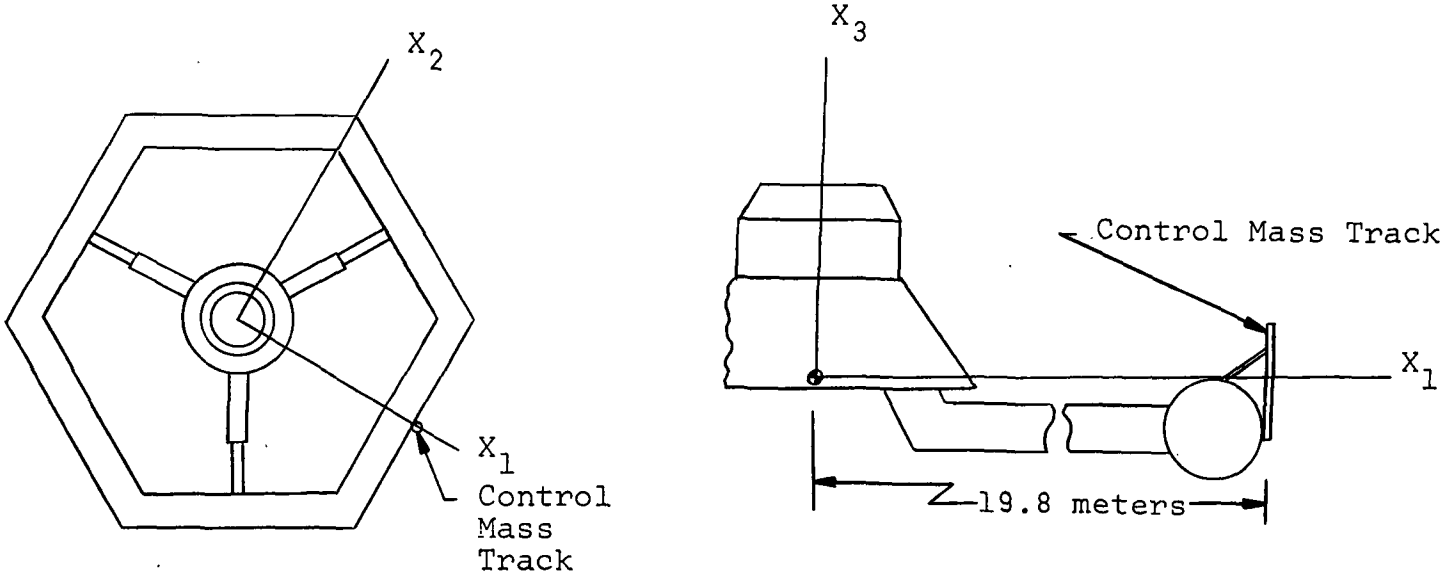

a) Plan View

b) Elevation

Figure 17. NASA 21 Man Space Station Configuration

vehicle will permit comparison of the movable mass system performance with the competitive devices identified by TRW.

The best performing passive damper identified by TRW is the controlled damping pendulum using three pendulum units, each with a tip mass of 272 kg (600 lbm). To match control system properties as closely as possible, the control mass weight for the movable mass system was selected as 816 kg (1,800 lbm). The wobble state considered by TRW was a wobble angle of five degrees which corresponds to the following initial conditions.

$$\omega_1(0) = 0.0391 \text{ radians/sec}$$

$$\omega_2(0) = 0$$

$$\omega_3(0) = 0.314 \text{ radians/sec}$$

The location of the control mass track is selected as shown in Figure 17. The values of track offset distances are

$$a = 19.8 \text{ meters (65 feet)}$$

$$b = 0$$

Based on these track offset distances and the stated initial conditions the control system parameters may be determined by the procedure given in the third section of Chapter III. From an analysis of the uncontrolled vehicle dynamics, the amplitude and frequency of the

forcing function of the mass equation of motion are determined as

$$D = 0.136 \text{ radians/sec}^2$$

$$p = 0.136 \text{ radians/sec}$$

Then using Equations 55 and 56 the control system constants may be determined.

$$c_2 = 0.0185 \text{ radians/sec}^2$$

$$c_1 = \frac{1}{z_{max}} \text{ radians/sec}$$

The performance of the control system was determined for maximum mass amplitudes of three-six meters, which were selected as typical values. Decay of the angle between the angular momentum vector of the system and the axis of symmetry of the vehicle is presented in Figure 18 for these cases. The wobble angle, θ, is defined as

$$\theta \triangleq \frac{I_1 \sqrt{\omega_1^2 + \omega_2^2}}{I_3 \omega_3}.$$

The values of c_1 corresponding to the selected maximum mass amplitudes and the resulting actual maximum amplitudes are summarized in Table III. It is interesting to note that the transient dynamics of the control system causes the mass to undershoot the predicted values of maximum amplitudes for these cases.

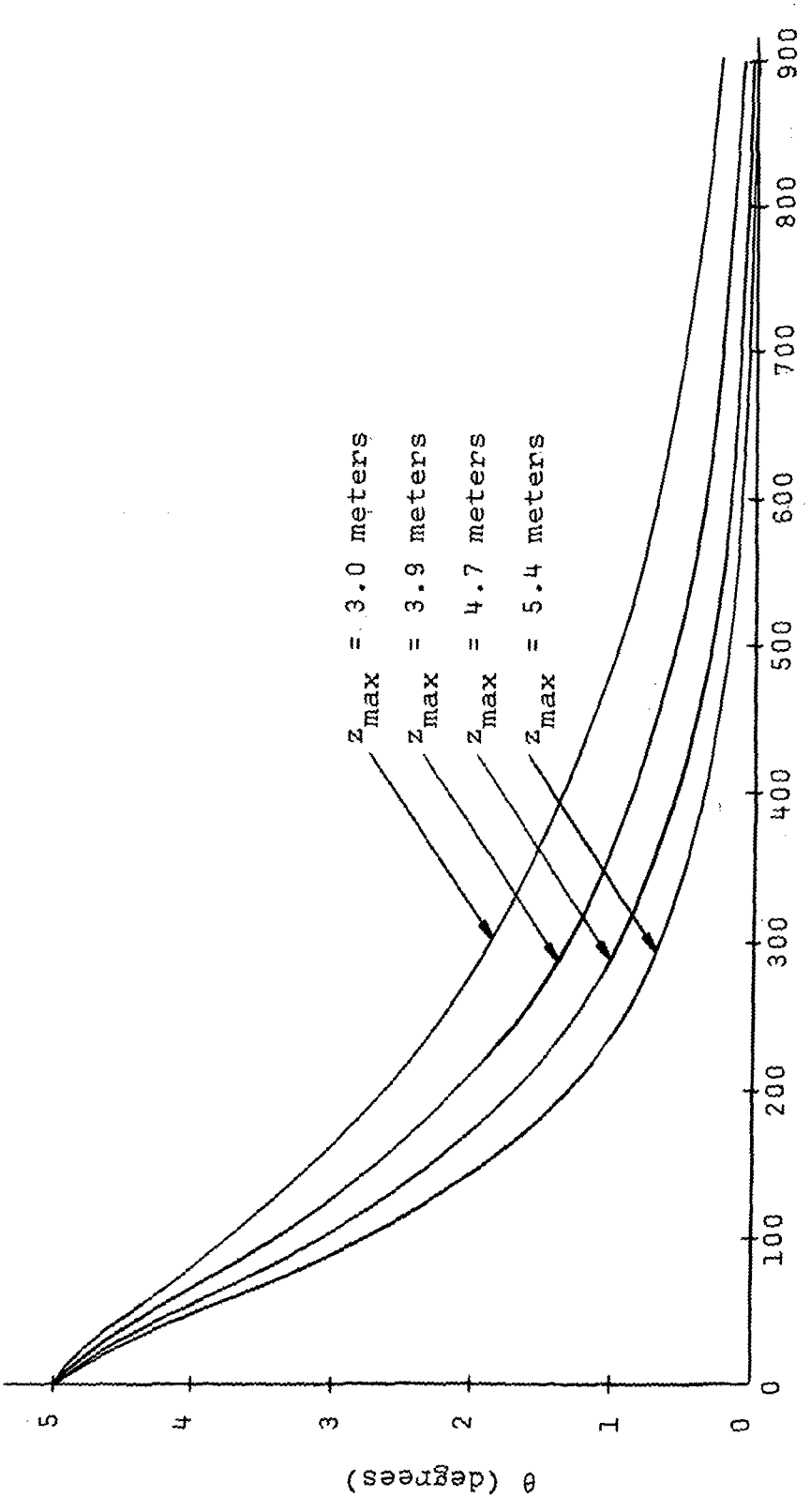

Figure 18. Performance of Control System as a Wobble Damper

Table III

Predicted and Actual Maximum Mass Amplitudes
for NASA 21 Man Space Station Simulation

c_1 (radians/sec)	z_{max} (meters) Predicted	Actual
0.333	3.0	3.0
0.250	4.0	3.9
0.200	5.0	4.7
0.167	6.0	5.4

The time constant, τ_c, is defined for a symmetric vehicle as the time required to reduce the wobble angle, θ, to a value of 1/e times its initial value. The resultant time constants, peak power, force, and energy requirements are summarized in Table IV for the cases considered. Also shown in the table are the time constants obtained by TRW for the passive devices they considered. With the exception of the case of $c_1 = 0.333$ ($z_{max} = 3$ meters), the movable mass control system produces faster stabilization than the passive damping devices identified by TRW. As shown in Table IV, the power, force, and energy requirements of the control system are modest. Thus, the feasibility of a movable mass control system as a wobble damper for a large artificial-g mode space station has been demonstrated.

Table IV

Wobble Damping Performance of Movable Mass and Competitive Systems

Device	τ_c (minutes)	Peak Power Required (watts)	Peak Force Required (newtons)	Required Energy (watt-sec)
Movable Mass System				
$c_1 = 0.334$	5.1	2.0	112.9	17.4
$c_1 = 0.250$	3.7	4.3	117.2	45.4
$c_1 = 0.200$	3.1	7.2	122.1	79.6
$c_1 = 0.167$	2.6	11.5	127.1	136.0
Controlled Damping Pendulum	3.8*			
Viscous Ring Damper	4.7*			
Pendulum Damper	5.3*			
NOTS Mercury Damper	≈100.0*			

*This data was obtained from Reference 12.

CHAPTER V

CONCLUSIONS

A movable mass control system has been conceived to convert the tumbling motions of a disabled vehicle into simple spin. It has been shown that a control law relating mass motion to vehicle motion may be formulated using Liapunov stability theory. This technique is useful for designing control systems where the governing equations of motion cannot be linearized.

For a large space station which is tumbling as a result of a collision with a shuttle orbiter, it has been shown that the movable mass system is capable of detumbling the space station within a period of two hours for the assumptions used. This is accomplished using a control mass weight of one percent of the vehicle weight and a mass amplitude of approximately three meters.

The following conclusions were drawn concerning control system design:

1. The mass track should be placed as far as possible from the vehicle center of mass and oriented parallel to the maximum moment of inertia axis.
2. The control mass weight should be selected as large as possible, consistant with peak force, power, and energy limitations.

3. The performance of the control system may be improved by allowing the mass to travel with a larger amplitude.

From the various cases considered, it can be concluded that the parameter selection procedure employed is valid and provides realistic estimates of parameter values.

As an additional application, it has been shown that the movable mass control system may be used as a wobble damper for a vehicle with an artificial-g mode. It has been determined that the performance for this system is better than competitive passive devices for this application.

In summary, the movable mass control system can effectively damp out unwanted tumbling or nutation motions of a large space vehicle with modest sensor, force, power, and energy requirements.

BIBLIOGRAPHY

1. Roberson, R. E., "Torques on a Satellite Vehicle from Internal Moving Parts," Transactions of the ASME, Journal of Applied Mechanics, Vol. 25, June, 1958, pp. 196-200.

2. Grubin, C., "Dynamics of a Vehicle Containing Moving Parts," Transactions of the ASME, Journal of Applied Mechanics, Vol. 29, September, 1962, pp. 486-488.

3. Kane, T. R., and Sobala, D., "A New Method for Attitude Stabilization," AIAA Journal, Vol. 1, No. 6, June, 1963, pp. 1365-1367.

4. Kane, T. R., and Scher, M. P., "A Method of Active Attitude Control Based on Energy Considerations," Journal of Spacecraft and Rockets, Vol. 6, No. 5, May, 1969, pp. 633-636.

5. Childs, D. W., "A Movable-Mass Attitude-Stabilization System for Artificial-g Space Stations," Journal of Spacecraft and Rockets, Vol. 8, No. 8, August, 1971, pp. 829-834.

6. Beachley, N. H., "Inversion of Spin-Stabilized Spacecraft by Mass Translation--Some Practical Aspects," Journal of Spacecraft and Rockets, Vol. 8, No. 10, October, 1971, pp. 1078-1080.

7. Lorell, K. R., and Lange, B. O., "An Automatic Mass-Trim System for Spinning Spacecraft," AIAA Journal, Vol. 10, No. 8, August, 1972, pp. 1012-1015.

8. Thomson, W. T., Introduction to Space Dynamics, John Wiley & Sons, New York, 1963.

9. La Salle, J. P., "Some Extensions of Liapunov's Second Method," IRE Transactions on Circuit Theory, December, 1960, pp. 520-527.

10. Synge, J. L., and Griffith, B. A., Principles of Mechanics, McGraw-Hill Book Co., Inc., New York, 1959, Chapters 13-14.

11. Kaplan, M. H., "Dynamics and Control of Escape and Rescue from a Tumbling Spacecraft," Semi-Annual Progress Report on NASA Grant NGR 39-009-210, Department of Aerospace Engineering, The Pennsylvania State University, December, 1971, pp. 7-50.

12. TRW Systems Engineering Mechanics Laboratory Staff, "Feasibility Study and Design of Passive Dampers for a Manned Rotating Space Station," NASA CR-163, March, 1965.